Theoret. Chim. Acta (Berl.) 60, 455–494 (1982)

THEORETICA CHIMICA ACTA

Intramolecular Electron–Hole Transfer in Binuclear Transition Metal Compounds–Theoretical Methods and Model Studies

Michael C. Böhm

Institut für Organische Chemie der Universität, Im Neuenheimer Feld 270, 6900 Heidelberg, Federal Republic of Germany

A theoretical framework for intramolecular electron or hole migration is developed starting from the convenient canonical molecular orbitals of an ordinary Hartree–Fock (HF) calculation. The necessary unitary transformations from the canonical MO basis via localized orbitals to a transfer Fockian are presented. A simple procedure for the consideration of relaxation and correlation effects during the time evolution is developed. Computational results for the hole migration between different metal $3d$ electron–hole pairs in bis(π-pentadienyl)dinickel (**1**) are discussed. The contribution of the direct transfer channel as well as the participation of ligand π and σ channels in the various propagation processes are analyzed.

Key words: Intramolecular electron (hole) propagation – Time-dependent perturbation theory – Binuclear transition metal systems.

1. Introduction

Intramolecular electron transfer events have been the subject of various experimental investigations and have been studied in bridged aromatic radicals [1, 2], in conducting organic polymers [3] as well as in polynuclear transition metal compounds. The most important examples in the organometallic field are mixed valence species [4–7], biochemical systems with transition metal centers as active sites (e.g. cytochromes) [8–10] and the transition metal derivatives that are able to convert light energy photochemically into chemical energy [11, 12]. Quantum-chemical procedures starting from first principles for the time evolution of the electron transfer processes are sparse.

0040-5744/82/0060/0455/$08.00

In this contribution we try to develop a theoretical framework for the time evolution of electron (hole) propagation in dimeric transition metal compounds starting from convenient Hartree–Fock (HF) orbitals as one-particle basis; the extension to other molecular arrangements is straightforward. The analysis is restricted to the purely electronical aspects, vibrational coupling is not considered in this investigation.

A detailed analysis based on time-dependent perturbation theory is given for the binuclear $3d$ complex bis(π-pentadienyl)dinickel (**1**) [13], a molecule clear enough that the various factors determining the transport properties can be discriminated in detail. The NiNi separation (2.59 Å) [14] lies in a range where the electron or hole propagation between the two $3d$ centers should be influenced both by the direct coupling and by the ensemble of available ligand transfer channels.

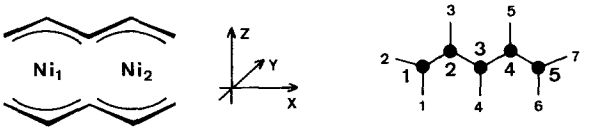

1 XY view

An investigation of the transport mechanisms in **1** seems of large interest in consideration of the recent effort to understand the catalytic and conducting properties of polynuclear organometallics [15].

The theoretical analysis is divided into different sections. In the following chapter the fundamental equations and the necessary theoretical limitations are presented. Additionally current models for intramolecular electron (hole) propagation are reviewed. In 3 the master equations for a hole transport in a dimeric system are derived. The transformation steps connecting the diagonal canonical molecular orbitals of an ordinary HF-ansatz with one-electron functions of a transport-type Hamiltonian are discussed in the fourth part. Refinements of the theory allowing the simulation of various conditions for the electron (hole) propagation are explained in the subsequent paragraph. In Sects. 6–8 the theoretical procedure is applied to bis(π-pentadienyl)dinickel.

Computational framework for the HF calculations and the subsequent time-dependent perturbational steps is a recently developed INDO-Hamiltonian [16] for transition metal compounds designed to reproduce *ab initio* results of double-zeta quality.

The theoretical and computational limitations presented in the following sections prevent the calculation of intramolecular transfer rates with an accuracy and a degree of sophistication that allows a direct comparison with experimentally derived quantities. Nevertheless we feel that our model studies give insight into the coupling mechanisms and interaction types between molecular fragments. Furthermore this is the first time-dependent approach starting from the convenient canonical MOs and therefore allows the introduction of the well known

static (time-independent) pictures of "through space" and "through bond" interaction [17].

2. Fundamental Equations and Review of Current Theoretical Approaches

The full Hamiltonian weakly coupled to a thermostat (e.g. low-frequency acoustical vibrations of the molecule or black body radiation) is given in Eq. (1)

$$H = H_{\mathrm{el}} + H_{\mathrm{v}} + H_{\mathrm{el\text{-}v}} + H_{\mathrm{vT}} + H_{\mathrm{T}}. \tag{1}$$

The individual components of H are defined by means of creation and destruction operators expressed in the representation of secondary quantization; a_i^+ and a_i are associated to the ith one-electron state while b_I^+ and b_I represent the creation-annihilation pair of the Ith molecular vibration.

H_{T} is the Hamiltonian of the thermostat and H_{vT} the Hamiltonian of the interaction molecule-thermostat. H_{T} and H_{vT} are responsible for energy dissipation during the transfer process and are not considered in the present investigation.

H_{v} symbolizes the vibrational Hamiltonian and $H_{\mathrm{el\text{-}v}}$ stands for the coupling between the one-electron states i and the molecular vibration I (electron-phonon interaction of the Fröhlich type) [18].

$$H_{\mathrm{v}} = \sum_I \hbar\omega_I (b_I^+ b_I + \tfrac{1}{2}) \tag{2}$$

$$H_{\mathrm{el\text{-}v}} = \sum_i \sum_I g_{iI} \hbar\omega_I a_i^+ a_i (b_I^+ + b_I). \tag{3}$$

The influence of H_{v} and $H_{\mathrm{el\text{-}v}}$ upon electron transfer phenomena depends on the relative timescale of the transfer process. If the electronical relaxation is faster than 10^{-14} sec (the shortest vibrational period in organic and organometallic systems) the probability of electron (hole) propagation is independent of H_{v} and $H_{\mathrm{el\text{-}v}}$. On the other hand dissipation times of instationary electron (hole) states exceeding this limit are strongly coupled to vibronic motions. The influence of H_{v} and $H_{\mathrm{el\text{-}v}}$ on electronic transfer events is not studied quantitatively in the present approach.

The electronic Hamiltonian H_{el} is defined in (4):

$$H_{\mathrm{el}} = \sum_i \sum_j h_{ij} a_i^+ a_j + \tfrac{1}{2} \sum_i \sum_j \sum_k \sum_l V_{ijkl} a_i^+ a_j^+ a_k a_l \tag{4}$$

h_{ij} stands for the one-electron contribution in H_{el} and V_{ijkl} symbolizes the two-electron part; both quantities are defined in (5) and (6) where $\{\varphi_i\}$ is any complete set of one-electron functions (orbitals)

$$h_{ij} = \langle \varphi_i(1) | -\tfrac{1}{2}\nabla^2 + h | \varphi_j(1) \rangle \tag{5}$$

$$V_{ijkl} = \left\langle \varphi_i(1)\varphi_j(2) \left| \frac{1}{r_{12}} \right| \varphi_k(1)\varphi_l(2) \right\rangle. \tag{6}$$

Making use of the Møller–Plesset theorem [19] (4) can be rearranged into (7) where the twofold summation i, j corresponds to the Hartree–Fock (HF) operator F^{AO} in the AO representation ($\{\varphi_i\}$ symbolizes the AO basis)

$$H_{el} = \sum_i \sum_j [h_{ij} + v_{ij}] a_i^+ a_j - \sum_i \sum_j v_{ij} a_i^+ a_j + \tfrac{1}{2} \sum_i \sum_j \sum_k \sum_l V_{ijkl} a_i^+ a_j^+ a_k a_l \tag{7}$$

$$v_{ij} = \sum_{l=1}^{occ} (V_{iljl} - V_{illj}) \tag{8}$$

$$F^{AO} = \sum_i \sum_j [h_{ij} + v_{ij}] a_i^+ a_j. \tag{9}$$

Diagonalization of F^{AO} results in the stationary delocalized canonical molecular orbitals (CMOs) where $\{\lambda_i\}$ represents the CMO basis

$$F^{CMO} = \sum_i \varepsilon_i a_i^+ a_i. \tag{10}$$

H_{el} therefore can be expressed by means of (11) and (12):

$$H_{el} = F^{CMO} + \tfrac{1}{2} \sum_i \sum_j \sum_k \sum_l V_{ijkl} a_i^+ a_j^+ a_k a_l \tag{11}$$

$$H_{el} = H_{el}^0 + H_{el}^{MB} \tag{12}$$

$$H_{el}^0 = F^{CMO} \tag{13}$$

$$H_{el}^{MB} = \tfrac{1}{2} \sum_i \sum_j \sum_k \sum_l V_{ijkl} a_i^+ a_j^+ a_k a_l. \tag{14}$$

H_{el}^{MB} goes beyond the quasiparticle picture of F^{CMO} taking into account many body interactions. The groundstate associated to F^{CMO} is symbolized by $|\phi_0\rangle$, the exact groundstate is given by $|\psi_0\rangle$. The groundstate determinant $|\phi_0\rangle$ can be formulated by means of any set of one-electron states $\{\varphi_i\}$ or $\{\lambda_i\}$ (CMOs) and does not depend on a concrete set of orbitals

$$|\phi_0\rangle = (N!)^{-1/2} |\varphi_1(1)\varphi_2(2) \cdots \varphi_N(N)| \tag{15}$$

$$|\phi_0\rangle = (N!)^{-1/2} |\lambda_1(1)\lambda_2(2) \cdots \lambda_N(N)|. \tag{16}$$

The molecular system determined by $|\phi_0\rangle$ ((15) or (16)) is completely described by the Hilbert space L_1^N mounted on any set of one-electron functions [20].

To study the time-dependency of electron or hole propagation one has to solve one of the Eqs. (17)–(19) with a properly chosen instationary, non-diagonal basis:

$$F|\phi_0(t)\rangle = i\hbar \frac{\partial}{\partial t} |\phi_0(t)\rangle \tag{17}$$

$$H_{el}|\psi_0(t)\rangle = i\hbar \frac{\partial}{\partial t} |\psi_0(t)\rangle \tag{18}$$

$$H_{\text{el,el-v}}|\psi_0(t)\rangle|I\rangle = i\hbar\frac{\partial}{\partial t}|\psi_0(t)\rangle|I\rangle \tag{19}$$

$$H_{\text{el,el-v}} = H_{\text{el}} + H_{\text{v}} + H_{\text{el-v}}. \tag{20}$$

Our investigations predominantly concern the time evolution formulated in (17) and (18). As the canonical MOs are no suitable choice for (17) or (18) the theoretical key step lies in the development of a unitary matrix M transforming the $\{\lambda_i\}$ set into a MO basis for a non-diagonal transport-type Fockian. If we are interested in the electron (hole) propagation from one localized, instationary state ρ_i to a second localized, instationary state ρ_j in the time period Δt, the following expressions for the HF determinant $|\phi_0(t)\rangle$ and for the Hilbert space $L_1^N(t)$ represent the suitable choice for time-dependent perturbation theory

$$|\phi_0(t)\rangle = A\{\rho_i(1,t)\rho_j(2,t)\gamma_1(3)\cdots\gamma_{(N-2)}(N)\} \tag{21}$$

$$L_1^N(t) = L_i(t) + L_j(t) + L_1^{(N-2)} \tag{22}$$

A is the antisymmetrization operator and γ represents a time-independent stationary one-electron basis belonging to a $(N-2)$ dimensional subspace. $L_i(t)$ and $L_j(t)$ symbolize the time-dependent Hilbert spaces mounted to the evoluting states $\rho_i(t)$ and $\rho_j(t)$ while $L_1^{(N-2)}$ is connected to the $(N-2)$ time-independent one-particle functions γ_k (messenger or transmitter orbitals).

None of the existing intramolecular electron (hole) transport theories is designed from first principles (e.g. HF SCF level) leading to an orbital representation suitable for the time evolution according to (21) and the Hilbert space relation (22). Current transfer theories can be classified into three categories (I, II, and III).

(I) The phenomenological tunnel electron transfer (TET) concept is based on the quasiclassical electron motion between two potential wells and has been developed for biological systems [8, 21]. In actual calculations the model parameters of the TET procedure are not calculated theoretically but they are determined by trial and error procedures to fit experimental data [21].

(II) Theoretical methods belonging to class II for the intramolecular electron (hole) transport are purely vibrational approaches where the electronic tunnel integral enters the working equations only parametrically as constant factor. These concepts have their origin in the classical Förster–Dexter equations [22] or are adopted from intermolecular transport theories [23–26]. The common drawback of the vibrational theories lies in the fact that they give no insight into electronical changes during the transfer process. They can be applied only in the time interval $>10^{-13}$–10^{-14} sec where the electron (hole) migration is strongly influenced by H_{v} and $H_{\text{el-v}}$ [27, 28].

(III) The third class of intramolecular electron transfer theories is based on the non-diagonal transport-type Hubbard–Hamiltonian [29] Eq. (23) with on-site Coulomb integrals γ_i and inter-site one-electron coupling elements β_{ij}

$$H_{\text{HU}} = \sum_{\sigma=\alpha}^{\beta}\sum_i\sum_j \beta_{ij}(a_{i\sigma}^+ a_{j\sigma} + a_{j\sigma}^+ a_{i\sigma}) + \sum_i \gamma_i n_{i\alpha} n_{i\beta} \tag{23}$$

$$n_{i\alpha} = a^{+}_{i\alpha} a_{i\alpha}$$

$$n_{i\beta} = a^{+}_{i\beta} a_{i\beta} \tag{24}$$

σ = spin variable α or β.

The Hubbard operator has been used in theoretical transfer studies in simple model systems [30].

The analytical structure of H_{HU} provides a suitable choice for a transport Fockian developed from the HF SCF level avoiding the approximative character of the Hubbard Hamiltonian.

Eqs. (10), (21), (22), and (23) suggest the following structure of the desired Fockian F^{HT}:

$$F^{\mathrm{HT}} = \sum_{i=i}^{j} \varepsilon_i a_i^{+} a_i + \sum_{\substack{k=1 \\ k \neq i,j}}^{\mathrm{occ}} \varepsilon_k a_k^{+} a_k$$

$$+ \sum_{i=i}^{j} \sum_{\substack{k=1 \\ k \neq i}}^{\mathrm{occ}} (\varepsilon_{ik} a_i^{+} a_k + \varepsilon_{ki} a_k^{+} a_i). \tag{25}$$

In (25) it is assumed that the hole propagation takes place between the ith and jth (donor state) localized instationary states, e.g. in the case of the Ni complex **1**: electron (hole) transfer between the transition metal centers.

A matrix representation of F^{HT} is displayed below.

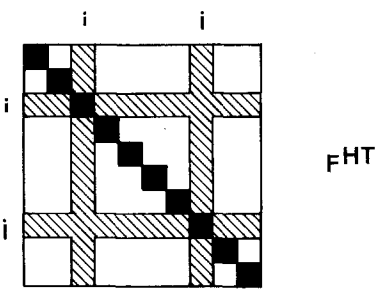

Scheme 1

i and j are the MO indices for the two localized one-electron functions ρ_i and ρ_j that take part in the transfer process. The diagonal elements ε_i and ε_j are associated to the localized domains; $\varepsilon_k (k \neq i, j)$ represent one-electron energies of the remaining $(N-2)$ orbitals. Each electron in the k set experiences the potential of $(N-3)$ electrons due to the ordinary HF averaging procedure and due to the decoupling of ρ_i and ρ_j. The life-times within the $(N-2)$ dimensional γ_k subset of course is infinite. The interaction between $\rho_i | \rho_j$ and γ_k is given by means of the cross-elements $\varepsilon_{ik} | \varepsilon_{jk}$; ε_{ij} obviously describes the direct coupling between the electron-hole pair. If a unitary transformation between (10) and (25) can be formulated, ε_i, ε_k and ε_{ik} contain kinetic energy, electron-core and

averaged electron-electron interaction within the HF picture and the coupling between the one-electron states is not of the phenomenological Hubbard type but related to standard LCAO procedures. Simplified versions of (25) have been formulated by various authors [31–33].

It is now straightforward to formulate the basis equations for time-dependent perturbation theory if once F^{CMO} has been transformed into F^{HT}

$$F^{\mathrm{HT}} = F_{\mathrm{D}}^{\mathrm{HT}} + F_{\mathrm{ND}}^{\mathrm{HT}} \tag{26}$$

$$F_{\mathrm{D}}^{\mathrm{HT}} = \sum_{i=i}^{j} \varepsilon_i a_i^+ a_i + \sum_{\substack{k=1 \\ k\neq i,j}}^{\mathrm{occ}} \varepsilon_k a_k^+ a_k \tag{27}$$

$$F_{\mathrm{ND}}^{\mathrm{HT}} = \sum_{i=i}^{j} \sum_{\substack{k=1 \\ k\neq i}}^{\mathrm{occ}} (\varepsilon_{ik} a_i^+ a_k + \varepsilon_{ki} a_k^+ a_i). \tag{28}$$

The time-independent determinantal wave function derived from (21) is given by (29) with the mixed $\{\rho_i, \gamma_k\}$ MO basis.

$$|\phi_0\rangle^{\mathrm{HT}} = (N!)^{-1/2} |\rho_i(1)\rho_j(2)\gamma_1(3)\cdots\gamma_{(N-2)}(N)|. \tag{29}$$

In the following $\{\rho_i, \gamma_k\}$ are collected into a common symbol $\{\gamma_i\}$. By means of the Dirac variation of constants [34] the time-dependent wave function developed from the $\{\gamma_i\}$ basis is obtained by the expansion (30) where the coefficients $a_i(t)$ have to be determined via Eq. (31)

$$\gamma_k(t) = \sum_i a_i(t)\gamma_i \tag{30}$$

$$(F_{\mathrm{D}}^{\mathrm{HT}} + F_{\mathrm{ND}}^{\mathrm{HT}})|\gamma_k(t)\rangle = i\hbar \frac{\partial}{\partial t}|\gamma_k(t)\rangle \qquad k = 1, 2, \ldots, N. \tag{31}$$

The $a_i(t)$ amplitudes are related to the time-independent $a_i(0)$ set ($t = 0$) due to the evolution operator U [35, 36]

$$a_i(t) = \sum_j U_{ij} a_j(0). \tag{32}$$

The probability for finding the initially prepared electron (hole) state in $\gamma_i (= \rho_i)$ at the time t is given in (33)

$$P_i(t) = |a_i(t)|^2 \tag{33}$$

$$P_i(t) = a_i^+(t) a_i(t) = \left(\sum_j U_{ij} a_j(0)\right)^+ \left(\sum_k U_{ik} a_k(0)\right)$$

$$= \sum_j |U_{ij}|^2 P_j(0) + \sum_j \sum_k U_{ij}^+ U_{ik} a_j^+(0) a_k(0). \tag{34}$$

In the framework of the random approximation (RPA) $P_i(t)$ is given by the simplified expression (35)

$$P_i(t) = \sum_j |U_{ij}|^2 P_j(0). \tag{35}$$

The probability of electron (hole) propagation within the one-electron pair ρ_i, ρ_j therefore is given by (36)

$$S_{ij}(t) = |U_{ij}|^2. \tag{36}$$

The investigation of the time evolution of (25)/(26) with the Hilbert relation (22) is traced back to the determination of U_{ij} for the instationary electron-hole pair $\rho_i|\rho_j$.

3. The Time Evolution of the Transport Type Fockian F^{HT}

According to Eq. (26) for F^{HT} the product-form (37) is used for the evolution operator

$$U = U_{\mathrm{D}} \cdot U_{\mathrm{ND}}. \tag{37}$$

U_{D} is associated to the diagonal Fockian $F_{\mathrm{D}}^{\mathrm{HT}}$ and U_{ND} corresponds to the perturbational operator $F_{\mathrm{ND}}^{\mathrm{HT}}$. U_{ND} is developed in the interaction representation [36] by means of Eq. (38) forming the basis equation of time-dependent perturbation theory [35]

$$U_{\mathrm{ND}} = \sum_{n=0}^{\infty} \left(-\frac{i}{\hbar}\right)^n \int_0^t dt \int_0^{t'} dt' \cdots \int_0^{t'^{(n-1)}} dt'^{(n-1)} \times F_{\mathrm{ND}}^{\mathrm{HT}}(t) \cdot F_{\mathrm{ND}}^{\mathrm{HT}}(t') \cdots F_{\mathrm{ND}}^{\mathrm{HT}}(t'^{(n-1)}). \tag{38}$$

$F_{\mathrm{ND}}^{\mathrm{HT}}(t)$ is determined by means of the transformation (39),

$$F_{\mathrm{ND}}^{\mathrm{HT}}(t) = U_{\mathrm{D}}^{+} F_{\mathrm{ND}}^{\mathrm{HT}} U_{\mathrm{D}} = \exp(iF_{\mathrm{D}}^{\mathrm{HT}} t|\hbar) F_{\mathrm{ND}}^{\mathrm{HT}} \exp(-iF_{\mathrm{D}}^{\mathrm{HT}} t|\hbar) \tag{39}$$

$$U_{\mathrm{D}} = \exp(iF_{\mathrm{D}}^{\mathrm{HT}} t|\hbar). \tag{40}$$

The matrix element U_{ij} in the one-electron basis (29) is given in (41)

$$\langle \rho_i | U | \rho_j \rangle = \exp(-i\varepsilon_i t|\hbar) \langle \rho_i | U_{\mathrm{ND}} | \rho_j \rangle. \tag{41}$$

The probability of electron (hole) propagation between $\rho_i|\rho_j$ therefore is determined by (42)

$$S_{ij}(t) = |\langle \rho_i | U_{\mathrm{ND}} | \rho_j \rangle|^2. \tag{42}$$

To solve (38) one has to evaluate the matrix elements of $F_{\mathrm{ND}}^{\mathrm{HT}}(t)$ in the interaction representation in analogy to the U_{ij} elements (Eq. (41))

$$\langle \rho_i | F_{\mathrm{ND}}^{\mathrm{HT}}(t) | \rho_j \rangle = \exp(i\omega_{ij} t) \langle \rho_i | F_{\mathrm{ND}}^{\mathrm{HT}} | \rho_j \rangle. \tag{43}$$

ω_{ij} is the Bohr frequency between the ith and jth diagonal element of $F_{\mathrm{D}}^{\mathrm{HT}}$

$$\omega_{ij} = (\varepsilon_i - \varepsilon_j)|\hbar. \tag{44}$$

In the case of the electron (hole) propagation $U_{\mathrm{ND}}(0)$ satisfies the (initial) condition $U_{\mathrm{ND}}(0) = 0$ due to the preparation of the electron (hole) state in ρ_i at $t = 0$.

The probability of hole propagation is related to the iterative expansion of Eq. (38); up to second order the following relation for $\langle \rho_i | U_{ND} | \rho_j \rangle$ is observed

$$\langle \rho_i | U_{ND} | \rho_j \rangle = (i\hbar)^{-1} \int_0^t dt \exp(i\omega_{ij}t)\varepsilon_{ij} - \left(\frac{1}{i\hbar}\right)^{-2} \sum_{\substack{k=1 \\ k\neq i,j}}^{\text{occ}} \int_0^t dt \int_0^{t'} dt' \exp(i\omega_{ik}t) \exp(i\omega_{kj}t)\varepsilon_{ik}\varepsilon_{jk}. \tag{45}$$

The restriction of the indices (j, k) is a result of the choice of the one-electron basis according to Eq. (29); the direct transfer channel is given by the first expression of (45), the k indirect propagation paths are determined by the second summation. According to the theoretical framework of R. Hoffmann and co-workers the coupling via ε_{ij} is called "through space" interaction [17] while the second order contributions with cross products $\varepsilon_{ik}\varepsilon_{kj}$ corresponds to the "through bond" interaction [17]. In the case of intramolecular electron (hole) propagation therefore the first order contribution to (45) can be assigned to a "through space" transfer channel while the indirect channels can be classified as "through bond" transfer.

The precise analytical form of the probability of hole propagation $S_{ij}(t)$ depends on possible resonance conditions between the one-electron states. In Fig. 1 the various possibilities are displayed. In **A** ρ_i, ρ_j as well as the messenger states(s) γ_k are degenerate, in **B** only the evoluting states have a vanishing Bohr frequency. In **C** and **D** a resonance condition between γ_k and one of the time-dependent states (ρ_i or ρ_j) is encountered while resonance conditions are absent in **E**.

The direct contribution to the probability of hole propagation in the case of a degeneracy between ρ_i and ρ_j is given in (46) and (47)

$$\langle \rho_i | U_{ND} | \rho_j \rangle_{RC}^{(1)} = (i\hbar)^{-1} \varepsilon_{ij} t \tag{46}$$

$$S_{ij}(t)_{RC}^{(1)} = \left(\frac{1}{\hbar}\right)^2 \varepsilon_{ij}^2 t^2 \tag{47}$$

RC = resonance condition.

In the case of the indirect second order channels **A** and **B** must be distinguished. The transfer quantities $\langle \rho_i | U_{ND} | \rho_j \rangle_{RC,RC}$ and $S_{ij}^{(2)}(t)_{RC,RC}$ are defined in (48) and (49)

$$\langle \rho_i | U_{ND} | \rho_j \rangle_{RC,RC}^{(2)} = \frac{1}{2}\left(\frac{1}{i\hbar}\right)^2 \varepsilon_{ik}\varepsilon_{kj} t^2 \tag{48}$$

$$S_{ij}^{(2)}(t)_{RC,RC} = \frac{1}{4}\left(\frac{1}{\hbar}\right)^4 \varepsilon_{ik}^2 \varepsilon_{kj}^2 t^4. \tag{49}$$

The second index in (48) and (49) remembers to the resonance condition (RC) for the direct coupling. The expressions for case **B** are determined by means

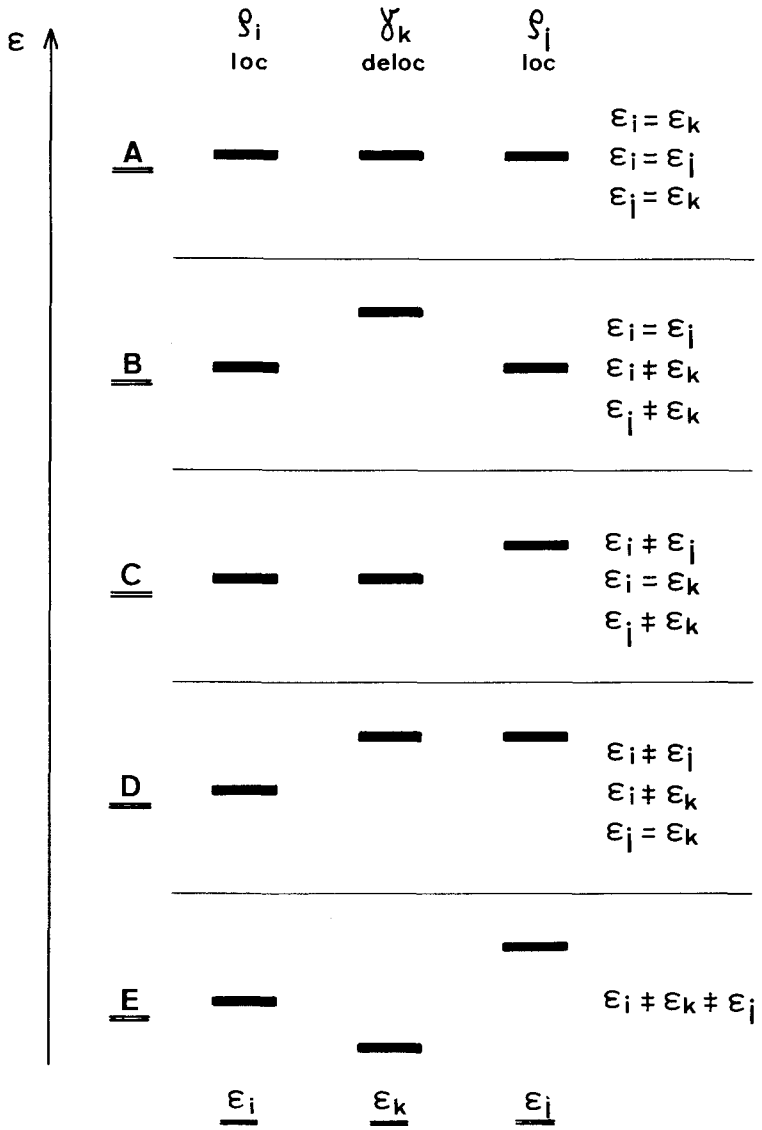

Fig. 1. Various possibilities for resonance conditions between the instationary, localized electron-hole pair ρ_i/ρ_j and the diagonalized orbitals γ_k coupled to ρ_i and ρ_j

of (50)–(52).

$$\langle\rho_i|U_{\mathrm{ND}}|\rho_j\rangle^{(2)}_{\mathrm{NRC,RC}} = \left(\frac{1}{i\hbar}\right)^2 \varepsilon_{ik}\varepsilon_{kj}\left(\frac{1}{i\omega_{ki}}\right) \times\left[\int_0^t dt' - \int_0^t dt' \exp\left(i\omega_{jk}t\right)\right] \tag{50}$$

(resonance between ε_i and ε_j)

$$\langle \rho_i | U_{\mathrm{ND}} | \rho_j \rangle^{(2)}_{\mathrm{NRC,RC}} = \left(\frac{1}{\hbar\omega_{jk}}\right) \varepsilon_{ik}\varepsilon_{kj}(i\omega_{ki}) \times \left[t - \left(\frac{1}{i\omega_{jk}}\right) \exp(i\omega_{jk}t) + \left(\frac{1}{i\omega_{jk}}\right)\right] \tag{51}$$

$$S_{ij}(t)^{(2)}_{\mathrm{NRC,RC}} = \left(\frac{1}{\hbar\omega_{ki}}\right)^2 \varepsilon^2_{ik}\varepsilon^2_{kj}(\omega_{ki})^2 \left\{ t^2 + 2\left(\frac{1}{\omega_{jk}}\right)^2 \times [1 - \cos(\omega_{jk}t) - (\omega_{jk})t \cdot \sin(\omega_{jk}t)]\right\} \tag{52}$$

NRC = non resonance condition.

Eqs. (47), (48) and (52) can be combined to the net probability of electron (hole) propagation (53) with a resonant direct transfer channel and resonant and non resonant indirect transfer paths

$$S_{ij}(t)_{\mathrm{tot,RC(1)}} = S_{ij}(t)^{(1)}_{\mathrm{RC}} + S_{ij}(t)^{(2)}_{\mathrm{RC,RC}} + S_{ij}(t)^{(2)}_{\mathrm{NRC,RC}}. \tag{53}$$

The first order quantities for the non resonant condition are defined in (54) and (55)

$$\langle \rho_i | U_{\mathrm{ND}} | \rho_j \rangle^{(1)}_{\mathrm{NRC}} = \left(\frac{1}{\hbar\omega_{ji}}\right) \varepsilon_{ij} [\exp(i\omega_{ij}t) - 1] \tag{54}$$

$$S_{ij}(t)^{(1)}_{\mathrm{NRC}} = \left(\frac{1}{\hbar\omega_{ji}}\right) \varepsilon^2_{ij} [2 - 2\cos(\omega_{ji}t)]. \tag{55}$$

In contrast to $S_{ij}(t)^{(1)}_{\mathrm{RC}}$ here the well-known oscillatory behaviour of the time-dependent perturbation theory is encountered [35–37].

In (56)–(58) the second order transfer quantities for $\varepsilon_i = \varepsilon_k$ and $\varepsilon_j \neq \varepsilon_k$ are derived; for **D** the indices i and j must be exchanged

$$\langle \rho_i | U_{\mathrm{ND}} | \rho_j \rangle^{(2)}_{\mathrm{RC,NRC}} = \left(\frac{1}{i\hbar}\right)^2 \varepsilon_{ik}\varepsilon_{jk} \int_0^t dt' \exp(i\omega_{jk}t')t' \tag{56}$$

$$\langle \rho_i | U_{\mathrm{ND}} | \rho_j \rangle^{(2)}_{\mathrm{RC,NRC}} = \left(\frac{1}{\hbar\omega_{jk}}\right)^2 \varepsilon_{ik}\varepsilon_{kj} [(i\omega_{jk}t)\exp(i\omega_{jk}t) - \exp(i\omega_{jk}t) + 1] \tag{57}$$

$$S_{ij}(t)^{(2)}_{\mathrm{RC,NRC}} = \left(\frac{1}{\hbar\omega_{jk}}\right)^4 \varepsilon^2_{jk}\varepsilon^2_{kj} \{(\omega_{jk}t)^2 + 2[1 - \cos(\omega_{jk}t) - (\omega_{jk}t)\sin(\omega_{jk}t)]\}. \tag{58}$$

In the case of the non resonating transfer channel the element (i, j) of the evolution operator is expressed via Eq. (59)

$$\langle \rho_i | U_{\mathrm{ND}} | \rho_j \rangle^{(2)}_{\mathrm{NRC,NRC}} = \left(\frac{1}{i\hbar}\right)^2 \varepsilon_{ik}\varepsilon_{kj}\left(\frac{1}{i\omega_{ki}}\right) \times \left\{\left(\frac{1}{i\omega_{ji}}\right)[\exp(i\omega_{ij}t)-1] - \left(\frac{1}{i\omega_{jk}}\right)[\exp(i\omega_{jk}t)-1]\right\}. \quad (59)$$

The probability of electron (hole) propagation for the NRC, NRC process is given in (60)

$$S_{ij}(t)^{(2)}_{\mathrm{NRC,NRC}} = \left(\frac{1}{\hbar}\right)^4 \left(\frac{1}{\omega_{ki}}\right)^2 \varepsilon^2_{jk}\varepsilon^2_{ki}\left\{\left(\frac{1}{\omega_{ji}}\right)^2 [2-2\cos(\omega_{ji}t)] + \left(\frac{1}{\omega_{jk}}\right)(2-2\cos(\omega_{jk}t)] - \left(\frac{1}{\omega_{ji}}\right)\left(\frac{1}{\omega_{jk}}\right)[2-2\cos(\omega_{jk}t) - 2\cos(\omega_{ji}t) + 2\cos(\omega_{kj}t)]\right\}. \quad (60)$$

(60) can be rearranged into (61) where the cos-functions with the same Bohr frequencies (ω_{ji}, ω_{jk} and ω_{ki}) are grouped together

$$S_{ij}(t)^{(2)}_{\mathrm{NRC,NRC}} = \left(\frac{1}{\hbar}\right)^2 \left(\frac{1}{\omega_{ki}\hbar}\right)^2 \varepsilon^2_{ik}\varepsilon^2_{kj}\left[\left(1-\frac{\omega_{ji}}{\omega_{jk}}\right) \times [2-2\cos(\omega_{ji}t)](\omega_{ji})^{-2} + \frac{(\omega_{ki})}{(\omega_{ji})}[2-2\cos(\omega_{jk}t)](\omega_{jk})^{-2} + \frac{(\omega_{ki})^2}{(\omega_{ji})(\omega_{jk})}[2-2\cos(\omega_{ki}t)](\omega_{kj})^{-2}\right]. \quad (61)$$

Using the $\delta(\varepsilon)$ representation (62) for the trigonometric expressions, (60) can be modified into Eq. (63)

$$\delta(\varepsilon) = \frac{\hbar^2}{2\pi\hbar t}[2-2\cos(\varepsilon t)](\hbar\varepsilon)^{-2} \quad (62)$$

$$S_{ij}(t)^{(2)}_{\mathrm{NRC,NRC}} = \frac{2\pi}{\hbar} t\left(\frac{1}{\omega_{ki}\hbar}\right)\varepsilon^2_{ik}\varepsilon^2_{kj}\left[\left(1-\frac{\omega_{ji}}{\omega_{jk}}\right)\cdot\delta(\hbar\omega_{ji}) + \frac{(\omega_{ki})}{(\omega_{ji})}\delta(\hbar\omega_{jk}) + \frac{(\omega_{ki})^2}{(\omega_{ji})(\omega_{jk})}\delta(\hbar\omega_{ki})\right]. \quad (63)$$

A relation similar to (61) already has been derived by Ratner and Ondrechen [33].

The complete set of transfer channels for $\varepsilon_i \neq \varepsilon_j$ is summarized in Eq. (64)

$$S_{ij}(t)_{\mathrm{tot,NRC(1)}} = S_{ij}(t)^{(1)}_{\mathrm{NRC}} + S_{ij}(t)^{(2)}_{\mathrm{RC,NRC}} + S_{ij}(t)^{(2)}_{\mathrm{RC,NRC}} + S_{ij}(t)^{(2)}_{\mathrm{NRC,NRC}} \quad (64)$$
$$(\varepsilon_k = \varepsilon_i) \qquad (\varepsilon_k = \varepsilon_j).$$

The explanation of the various increments in (64) is straightforward; the first term stands for the direct coupling under non resonant propagation conditions, the second and third correspond to resonance between γ_k and $\rho_i|\rho_j$ while the last element refers to non resonant conditions between $\rho_i|\rho_j$ and the transmitter set γ_k.

4. The Transformation of the Canonical Fock Matrix into a Hubbard-Type Transport Fockian

For the unitary transformation between the CMO representation (10) and the HF representation (25) it is assumed that a closed shell HF determinant with paired spins is given. We furthermore assume that reorganization effects in the vicinity of the localized hole-state ρ_i can be neglected, an approximation similar to Koopmans' theorem [38] in the field of photoelectron spectroscopy. Refinements of this independent electron model due to relaxation and correlation are introduced in the next section. The advantage of the present approach lies in the fact that the closed shell orbitals can be used in the transformation steps. Additionally the capability of the virtual MO space as transmitter set is neglected.

The intended reformulation of the HF problem from Eq. (10) into (25) can be achieved by a series of transformations properly modified from a thematically related approach developed by Heilbronner and Schmelzer [39].

In the first step the canonical molecular orbitals $\{\lambda_i\}$ associated to F^{CMO} are transformed into a set of localized orbitals $\{\rho_1, \rho_2 \cdots \rho_N\}$ and to the Fock operator F^{LMO} which is a full matrix (65). Possible choices for the transformation matrix L connecting $\{\lambda_i\}$ with $\{\rho_i\}$ are discussed below; often this selection is by no means trivial

$$F^{\mathrm{LMO}} = \sum_{i}^{\mathrm{occ}} \varepsilon_i a_i^+ a_i + \sum_{i \neq j}^{\mathrm{occ}} \sum^{\mathrm{occ}} (\varepsilon_{ij} a_i^+ a_j + \varepsilon_{ji} a_j^+ a_i) \tag{65}$$

(the associated one-particle basis $\{\rho_i\}$)

$$\mathbf{L}\lambda = \rho \tag{66}$$

$$\mathbf{F}^{\mathrm{LMO}} = \mathbf{L}\mathbf{F}^{\mathrm{CMO}}\mathbf{L}^T. \tag{67}$$

Within the LMO representation ρ_i and ρ_j with their associated diagonal Lagrange multiplicators have the desired properties of the time-evoluting electron-hole pair. Decoupling of ρ_i and ρ_j from F^{LMO} results in the decoupled Fockian (68) schematically displayed in Scheme 2. The off-diagonal elements in row and column i, j are set equal to zero.

$$F^{\mathrm{LMO}}_{(i,j)\mathrm{DEC}} = \sum_{i=i}^{j} \varepsilon_i a_i^+ a_i + \sum_{\substack{k=1 \\ k \neq i,j}}^{\mathrm{occ}} \varepsilon_k a_k^+ a_k + \sum_{\substack{k=1 \\ k \neq i,j,l \neq i,j}}^{\mathrm{occ}} \sum_{\substack{l=1 \\ l \neq k}}^{\mathrm{occ}} (\varepsilon_{kl} a_k^+ a_l + \varepsilon_{lk} a_l^+ a_k). \tag{68}$$

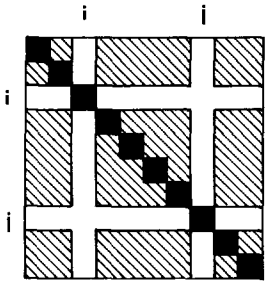

Scheme 2

The off-diagonal pattern of $F^{\mathrm{LMO}}_{(i,j)\mathrm{DEC}}$ is just the "negative" of the ε_{ij} distribution in F^{HT}. To determine F^{HT} the Fockian (68) is diagonalized. The eigenvectors of $F^{\mathrm{LMO}}_{(i,j)\mathrm{DEC}}$, D_{ij}, transform the localized MO set $\{\rho_i\}$ into the mixed one-particle representation $\{\gamma_i\}$ (Eq. 69) and F^{HT} is obtained via the matrix transformation (70)

$$\gamma = \mathbf{D}_{ij}\rho \tag{69}$$

$$\mathbf{F}^{\mathrm{HT}} = \mathbf{D}_{ij}\mathbf{F}^{\mathrm{LMO}}\mathbf{D}^{\mathrm{T}}_{ij}. \tag{70}$$

Eqs. (67) and (70) can be unified in (71) leading to the transformation matrix M connecting the diagonal CMO basis with the mixed one-electron basis of F^{HT}

$$\mathbf{F}^{\mathrm{HT}} = \mathbf{D}_{ij}\mathbf{L}\mathbf{F}^{\mathrm{CMO}}\mathbf{L}^{\mathrm{T}}\mathbf{D}^{\mathrm{T}}_{ij} \tag{71}$$

$$\mathbf{M} = \mathbf{D}_{ij}\mathbf{L} \tag{72}$$

$$\mathbf{F}^{\mathrm{HT}} = \mathbf{M}\mathbf{F}^{\mathrm{CMO}}\mathbf{M}^{\mathrm{T}}. \tag{73}$$

The design of various other choices for the one-electron bases, the mounted Hilbert spaces and the necessary transformations is explained in Appendix A.

The technical important step for the construction of F^{HT} consists in the determination of the transformation matrix L. Only in a narrow class of molecules this transformation can be performed by means of intrinsic localization routines [40] that only depend on the selected HF SCF basis. Intrinsic localization procedures have been developed by various authors [41–43]. In the case of the Edmiston–Ruedenberg algorithm [41] e.g. the self-energy integrals (74) are maximized

$$\sum_{i=1}^{\mathrm{occ}} \left(\left\langle \rho_i(1)\rho_i(2) \left| \frac{1}{r_{12}} \right| \rho_i(1)\rho_i(2) \right\rangle \right) = \text{maximum}. \tag{74}$$

Intrinsic localization routines cannot be applied in molecules with lone-pair combinations, localized metal d orbitals and moieties with an uneven number of AOs. As the Fockian of dimension N is identified by $N(N-1)/2$ independent parameters (N parameters satisfy the energy spectrum, $(N-1)/2$ are used for the representation of the eigenfunctions) it is always possible to restrict the available degrees of freedom by external conditions. A constrained localization procedure has been developed by Magnasco and Perico [44] accumulating the orbital electron density in preselected regions of the molecule by means of the

localization function P

$$2P = \sum_{o} 2P_o = \text{maximum} \qquad o \in \{\text{occ}\} \tag{75}$$

$$2P_o = 2 \sum_{\mu} \sum_{\nu} c_{\mu o} c_{\nu o} 0_{\mu\nu}. \tag{76}$$

The summation runs through the orbitals of a preselected set; P_o is the local orbital population, μ and ν are AO indices, $0_{\mu\nu}$ the associated overlap integral and $c_{\mu o}$, $c_{\nu o}$ the usual LCAO coefficients. Various choices for P_o in the case of core orbitals, lone-pair and bonds are discussed in Ref. [44]. Metal $3d$ orbitals are treated in the same way as core orbitals and lone-pairs.

In the present work we have combined the organizational simplicity of the intrinsic Edmiston–Ruedenberg (ER) procedure with necessary restrictions defined via external conditions according to Magnasco and Perico (MP) avoiding the difficult complete implementation of the latter method in the case of large MO spaces.

The coupled localization procedure (ER/MP) requires the selection of a subspace $\{\lambda_i\}_{MP}$ out of the full canonical MO space where the external MP conditions are applied for the accumulation of orbital density in preselected molecular domains. In a subsequent step the whole MO set (prelocalized MO's of the $\{\lambda_i\}_{MP}$ space and the remaining MO's) is transformed by means of the ER procedure. It is always checked that the domains of $\{\lambda_i\}_{MP}$ are conserved; both localization types are applied alternatingly up to convergence.

5. The Influence of Relaxation and Correlation

In Sect. 3 it has been demonstrated that the probability of hole propagation is critically influenced by resonating or non resonating transfer channels. In the case of a molecule with identical centers forming the $\rho_i|\rho_j$ pair the use of an independent electron model always results in a resonating direct channel. Relaxation and correlation in the ith hole-domain on the other hand cause deviations from the independent electron approach. To take into account these reorganizational rearrangements in the evoluting states we make use a theoretical method related to Slater's transition state theory developed in the X_α approximation [45] and transferred to the transition operator method as LCAO counterpart [46].

Reorganizational rearrangements for the ith prepared hole-state and the time-dependent electron-state ρ_j are considered by means of the Δ_i potential (see below)

$$\varepsilon_i(t_n) = \varepsilon_i(t_{n-1}) + (1 - S_{ij}(t_{n-1}))\Delta_i \tag{77}$$

$$\varepsilon_j(t_n) = \varepsilon_j(t_{n-1}) + S_{ij}(t_{n-1})\Delta_i. \tag{78}$$

(77) and (78) obey the rule of conservation of energy. At $(S_{ij}(0) = 0)$ the prepared hole-state alone is influenced by the Δ_i potential. With increasing time the

reorganization in the ρ_i domain is asymptotically reduced while a new Δ_i potential is created in the jth donor state.

For the determination of Δ_i we have used a relation developed by Gopinathan [47] connecting the reorganization Δ_i with the self-energy of the ρ_ith state

$$\Delta_i = c_i \left\langle \rho_i(1)\rho_i(2) \left| \frac{1}{r_{12}} \right| \rho_i(1)\rho_i(2) \right\rangle. \tag{79}$$

Eq. (79) holds in the case of full electron (hole) localization. The proportionality constant c_i has been observed by means of sample calculations where Δ_i is related

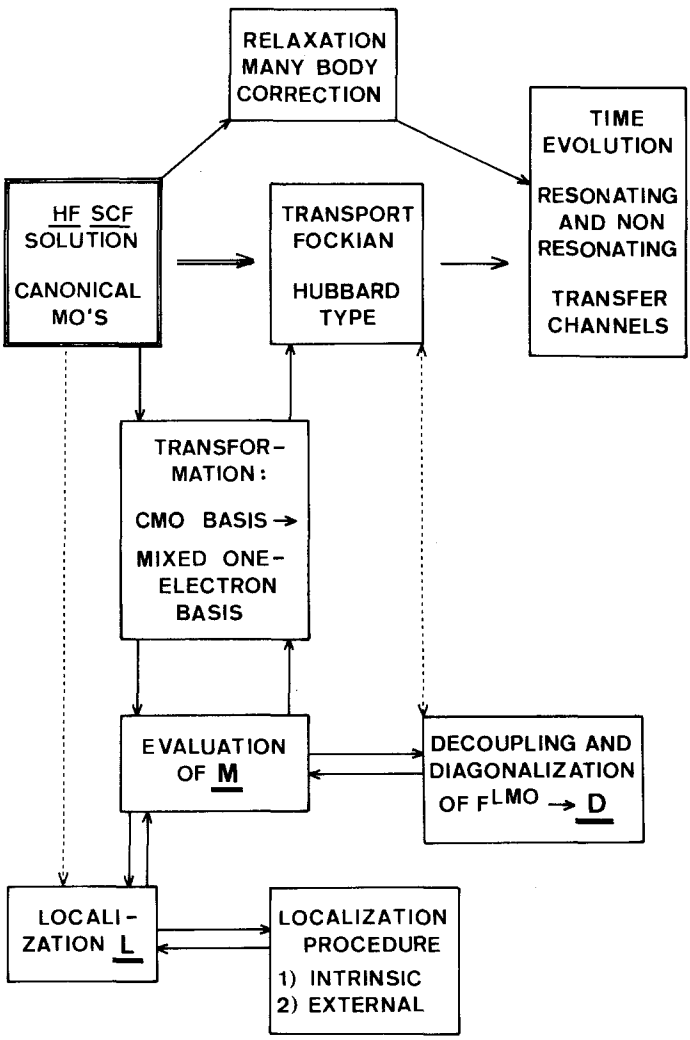

Fig. 2. Schematical interrelation between the various theoretical steps for the calculation of intramolecular hole (electron) migration

to a renormalized approximation of the self energy part in a Green's function approach [48] $\Sigma(\omega_i)^{\text{eff}}$. $\Sigma(\omega_i)^{\text{eff}}$ contains deviations from the independent particle energies ε_i due to relaxation and correlation. The renormalized $\Sigma(\omega_i)^{\text{eff}}$ ansatz has been developed by Cederbaum [49] for one-particle states in the outer valence region

$$\Delta_i = \Sigma(\omega_i)^{\text{eff}} = \Sigma^{(2)}(\omega_i)_{ii} + D4_{ii}. \tag{80}$$

Eqs. (79) and (80) can be unified for the determination of c_i in some test calculations which together with the known integrals in (79) can be used in (77) and (78). Further details are given in Appendix B.

A generalization of Eq. (79) is formulated in Eq. (81) where the k parameter allows the modification of the initially prepared reorganization energies at $t = 0$ in the ith hole domain

$$\Delta_i = (1-k)c_i\left\langle \rho_i(1)\rho_i(2)\left|\frac{1}{r_{12}}\right|\rho_i(1)\rho_i(2)\right\rangle. \tag{81}$$

In the limit $k = 1$ an independent electron model is realized. With reduced k values reorganizational rearrangements in the evoluting states are taken into account. If $k = 0$ the ith hole-domain is completely reorganized. By means of (79) and (81) therefore it is possible to go beyond the HF picture in the treatment of electron (hole) propagation; the use of the Δ_i potential offers an opportunity to study the time evolution based on an approximation of Eq. (18).

In Fig. 2 the necessary theoretical steps for the intramolecular electron (hole) propagation problem are summarized. Starting point are the canonical MO's of an ordinary HF SCF calculation. The CMO representation is connected via the matrix M to the Fockian of the Hubbard type. The selection of the localization routine (L) is independent from the structure of F^{HT}; the necessary decoupling steps (D) depend on the investigated time-dependent problem. The Δ_i corrections are used directly in the equations for the various transfer channels.

6. The Canonical Representation of Bis(π-pentadienyl)dinickel

In Table 1 the canonical MO energies of **1** according to the INDO model are summarized. The most important interactions between the Ni $3d$ orbitals and the ligand π functions are displayed in Fig. 3. Atomic populations and net charges [50] as well as Wiberg bond indices [51] are collected in Tables 2 and 3.

The MO's 1–4 are CC-σ ligand functions with predominant C $2s$ character; 13, 18, 19 and 21 are σ-ribbon orbitals with large C $2p$ amplitudes. 5–12, 14–16, 20, 22 and 23 correspond to CH-σ orbitals of the pentadienyl ligands.

For the MO's $8a_g$, $8b_u$, $7a_u$, $9a_g$ and $8a_u$ Ni $3d$ contributions larger than 95% are predicted. These orbitals correspond to in-phase and out-of-phase combinations of the Ni $3d$ AO's $3d_{z^2}$, $3d_{x^2-y^2}$ and $3d_{xy}$ (in-phase only). Significant interactions between $3d_{xz}$ and $3d_{yz}$ and ligand π functions are predicted. Table 1 indicates that the metal ligand coupling via $3d_{xz}$ exceeds the interaction via $3d_{yz}$.

Table 1. Canonical molecular orbitals of bis(π-pentadienyl)dinickel **1** according to an INDO calculation. The orbital energies, ε_i, are given in eV. The Ni, the pentadienyl ligand carbon and hydrogen contribution, the type as well as the irreducible representation (Γ_i) of the MO wave function are indicated. The numbering scheme of the Γ_i values corresponds to the valence-electron distribution, the core electrons are not explicitly taken into account. MLI symbolizes the metal ligand interaction; B is a bonding and AB an antibonding coupling. FI symbolizes the fragment interaction (Ni_1Ni_2 coupling, interaction between the pentadienyl ligands); IP stands for an in-phase relation while OP symbolizes the out-of-phase interaction of the fragments. P = pentadienyl ligand

MO	Γ_i	MO-type	ε_i(eV)	MLI	FI[a]	% Ni	% C(P)	% H(P)
1	$1a_g$	CC-$\sigma(s)$	−41.31			2.4	82.9	14.7
2	$1b_u$	CC-$\sigma(s)$	−39.80			2.1	83.4	14.5
3	$1a_u$	CC-$\sigma(s)$	−36.78			1.9	80.0	18.1
4	$1b_g$	CC-$\sigma(s)$	−34.59			0.8	82.2	17.0
5	$2a_g$	CH-σ	−28.97			0.7	74.9	24.4
6	$2b_u$	CH-σ	−27.45			0.5	76.8	22.7
7	$3b_u$	CH-σ	−24.50			0.6	58.5	40.9
8	$3a_g$	CH-σ	−24.13			0.6	59.4	40.0
9	$2a_u$	CH-σ	−22.42			0.6	67.0	32.4
10	$2b_g$	CH-σ	−21.73			0.5	62.8	36.7
11	$3a_u$	CH-σ	−19.70			2.0	67.9	30.1
12	$3b_g$	CH-σ	−19.65			0.2	71.7	28.1
13	$4a_g$	CC-$\sigma(p)$	−17.13			1.2	85.0	13.8
14	$4b_u$	CH-σ	−16.91			1.0	77.7	21.3
15	$5a_g$	CH-σ, $3d_{yz}$	−16.15	B		6.4	65.7	27.9
16	$5b_u$	CH-σ	−15.79			2.7	59.8	37.5
17	$6a_g$	CC-$\pi(\pi_1)$, $3d_{yz}$	−14.79	B	IP	6.4	78.1	15.5
18	$4a_u$	CC-$\sigma(p)$, $3d_{yz}$	−14.35	B		5.8	73.7	20.5
19	$4b_g$	CC-$\sigma(p)$	−14.25			2.3	80.0	17.7
20	$5b_g$	CH-σ, $3d_{xz}$	−13.73	B		8.6	63.8	27.6
21	$5a_u$	CC-$\sigma(p)$, $3d_{yz}$	−13.66	B		5.3	79.2	15.5
22	$7a_g$	CH-σ, $3d_{yz}$	−13.53	B		7.0	59.0	34.0
23	$6b_u$	CH-σ	−13.42			0.6	65.4	34.0
24	$6a_u$	CC-$\pi(\pi_2)$, $3d_{yz}$	−13.16	B	IP	25.2	64.7	10.1
25	$7b_u$	CC-$\pi(\pi_1)$	−12.75		OP	2.5	95.5	2.0
26	$6b_g$	$3d_{xy}$, CC-$\pi(\pi_3)$	−11.55	B	OP	48.6	51.1	0.3
27	$8a_g$	$3d_{x^2-y^2}$	−11.46		IP	97.3	2.4	0.3
28	$8b_u$	$3d_{xy}$	−11.45		IP	95.9	3.8	0.3
29	$7a_u$	$3d_{x^2-y^2}$	−11.42		OP	97.1	2.7	0.2
30	$9a_g$	$3d_{z^2}$	−11.40		IP	97.0	2.0	1.0
31	$8a_u$	$3d_{z^2}$	−11.37		OP	97.6	1.6	0.8
32	$7b_g$	$3d_{xz}/3d_{xy}$, CC-$\pi(\pi_2)$	−11.37	AB	OP	72.5	25.9	1.6
33	$9b_u$	$3d_{xz}$, CC-$\pi(\pi_3)$	−11.21	B	IP	55.5	43.3	1.2
34	$10a_g$	$3d_{yz}$, CC-$\pi(\pi_1)$	−10.61	AB	IP	79.9	17.9	2.2
35	$9a_u$	$3d_{yz}$, CC-$\pi(\pi_2)$	−10.22	AB	OP	62.6	35.8	1.6
36	$8b_g$	$3d_{xz}$, CC-$\pi(\pi_2)$	−8.89	AB	OP	55.1	43.7	1.2
37	$11a_g$	CC-$\pi(\pi_3)$	−8.73		IP	0.7	99.1	0.2

[a] The symbol (IP/OP) in the FI-column always corresponds to the fragment interaction which contributes predominantly to the MO's.

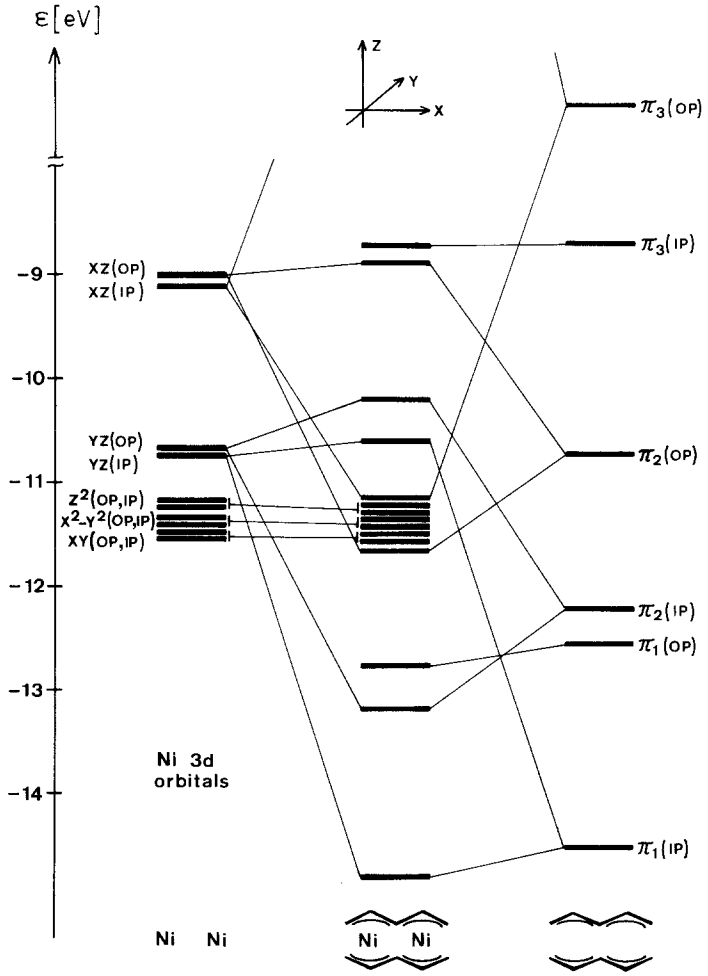

Fig. 3. Interaction diagram between the Ni $3d$ orbitals of the Ni_1Ni_2 moiety and the π-orbitals of the pentadienyl ligands; the $3d$ orbitals of the Ni centers are split due to the interaction with the σ-frame of the ligands. IP = in-phase, OP = out-of-phase

This difference is rationalized on the basis of the Ni $3d$ populations in Table 2 and the bond indices in Table 3. Large Ni AO populations are predicted for $3d_{z^2}$, $3d_{x^2-y^2}$, $3d_{xy}$ and $3d_{yz}$ (1.9e) while the $3d_{xz}$ population is significantly reduced (1.6e). The NiNi bond index of Table 3 shows that the direct coupling between the $3d$ centers is only of minor importance. The bond indices in the pentadienyl framework predict a remarkable bond localization in the region of the terminal C atoms (C_1C_2 and C_4C_5); this is also seen in the charge accumulation between these centers.

The INDO results collected in Tables 1–3 suggest the following decoupling of Ni $3d$ states for the investigation of an intramolecular hole transfer: $3d_{z^2}$, $3d_{x^2-y^2}$,

Table 2. Atomic populations and net charges of bis(π-pentadienyl)dinickel **1** according to an INDO calculation

AO	Ni_1=Ni_2	AO	C_1=C_5	C_2=C_4	C_3	AO	H_1=H_6	H_2=H_7	H_3=H_5	H_4
$4s$	0.0425	$2s$	1.1215	1.0415	1.0492	$1s$	0.8774	0.8520	0.8741	0.8719
$4p_x$	0.0221	$2p_x$	1.0651	1.0215	1.0045					
$4p_y$	0.0164	$2p_y$	1.0473	1.0517	1.0745					
$4p_z$	0.0263	$2p_z$	1.2144	1.0000	1.2121					
$3d_{z^2}$	1.9979									
$3d_{xz}$	1.5960									
$3d_{yz}$	1.9732									
$3d_{x^2-y^2}$	1.9182									
$3d_{xy}$	1.8622									
Net charge	0.5452		−0.4484	−0.1147	−0.3402		0.1226	0.1480	0.1259	0.1281

Table 3. Wiberg bond indices for bis(π-pentadienyl)-dinickel **1** according to an INDO calculation

Bond	Bond index
Ni_1Ni_2	0.0891
$Ni_1C_1{=}Ni_2C_5$	0.2483
$Ni_1C_2{=}Ni_2C_4$	0.1097
$Ni_1C_3{=}Ni_2C_3$	0.1457
$C_1C_2{=}C_4C_5$	1.5817
$C_2C_3{=}C_3C_4$	1.2289
$C_1C_3{=}C_3C_5$	0.0212
C_2C_4	0.0053

$3d_{xy}$ and $3d_{yz}$. Due to the strong interaction between the Ni $3d_{xz}$ AOs and the π functions of the ligands the decoupling of these $3d$ functions is without any significance; the Ni $3d_{xz}$ AOs are used for the formation of two localized five

center bounds (see above). In the localized MO representation these two linear combinations are forming the transition metal-carbon bonds. Localized π orbitals should be constructed between the terminal carbon centers.

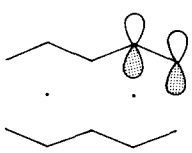

The localization of CC-σ and CH-σ causes no problems. The remaining occupied MO of **1** in a localized representation is a nonbonding π combination where the interaction with Ni $3d$ is prevented due to symmetry.

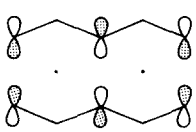

It is clear that this localization pattern cannot be obtained by an intrinsic localization procedure.

7. The Hubbard-Type Representation of Bis(π-pentadienyl)dinickel

In Table 4 the various types of localized orbitals of **1** together with the diagonal Lagrange multiplicators and impurities from other atomic centers are collected. The ligand CC-σ and CH-σ orbitals are strongly localized; this is also found

Table 4. Localized molecular orbitals of bis(π-pentadienyl)dinickel **1**. Type, number and localization properties of the localized MO's are also indicated. The diagonal elements ε_i^{LMO} are given in eV

MO-Type	ε_i^{LMO}	Number	Impurities %
CC-σ(C_2C_3=C_3C_4)	−24.12	4	0.7
CC-σ(C_1C_2=C_4C_5)	−24.04	4	1.1
CH-σ(C_3H_4)	−21.16	2	0.9
CH-σ(C_1H_1=C_5H_6)	−21.09	4	1.0
CH-σ(C_1H_2=C_5H_7)	−20.91	4	0.3
CH-σ(C_2H_3=C_4H_5)	−20.86	4	0.4
CC-π(C_1C_2=C_4C_5)	−12.30	4	8.7
Ni $3d_{z^2}$	−11.51	2	0.1
Ni $3d_{yz}$	−11.48	2	1.4
Ni $3d_{x^2-y^2}$	−11.45	2	4.1
Ni $3d_{xy}$	−11.44	2	2.7
nonbonding π-MO delocalized, in-phase	−11.05	1	18.1
$Ni_1 3d_{xz}$-C_1C_3=$Ni_2 3d_{xz}$-C_3C_5	−10.86	2	10.5

for Ni $3d_{z^2}$, $3d_{x^2-y^2}$ and $3d_{xy}$ functions. The impurities in most of the localized MO's are less than 1%. The π functions in the ρ_i representation show surprisingly pronounced localization properties (8.7% impurities). Similar impurity contributions are predicted for the two localized Ni carbon multicenter bonds.

In Tables 5 and 6 the diagonal elements as well as the coupling terms of the Hubbard-type Fockian are summarized; the theoretical transformations have been discussed in Sect. 4. Always two Ni $3d$ AOs (localized) were decoupled. In Table 5 the interaction elements for eight localized ρ_i states with the remaining 29 symmetryadapted (pointgroup C_{2h}) time-independent messenger orbitals are displayed. The descent of the γ_i subspace from the canonical representation (Table 1) is clearly recognized. Negligible energy shifts are found in those ligand combinations where only small Ni $3d$ contributions were concerned in the CMO's.

None of the Ni $3d$ ligand interaction elements ("transfer integrals") exceeds 1 eV, most of the cross-elements are significantly smaller. For the decoupled $3d_{z^2}$ set remarkable interaction constants with CC-σ (MO 1 and 3) and CH-σ (MO 8, 12 and 15) messenger states are predicted. The interaction terms with ligand π combinations are less than 0.1 eV. In the case of the two localized $3d_{yz}$ orbitals the most pronounced off-diagonal elements are calculated.

It is seen that all types of ligand messenger states (CC-π, CC-σ and CH-σ) are effectively coupled to the transition metal AOs, the transfer determining factor therefore is the magnitude of the Bohr frequencies. The smallest Ni $3d$ ligand coupling elements are predicted for $3d_{x^2-y^2}$ and $3d_{xy}$.

In Table 6 the direct interaction elements between the Ni centers are summarized ("through space" coupling). These elements are small in comparison to the various nickel pentadienyl interaction constants. Nevertheless a graduation

Table 5. Molecular orbitals of bis(π-pentadienyl)dinickel in the Hubbard-type representation where the $3d_{z^2}$, $3d_{yz}$, $3d_{x^2-y^2}$ and $3d_{xy}$ AOs of Ni_1 and Ni_2 have been decoupled from the canonical MO ensemble. The diagonal elements and the interaction elements of the Fock matrix are given; all values in eV. loc stands for the decoupled Ni $3d$ function, the remaining orbitals transform according to the irreducible representations of the molecular point group (C_{2h})

				Coupling constants							
MO	Γ_i	MO-Type	ε_i^{HT}	$3d_{z^2}$ 1	$3d_{z^2}$ 2	$3d_{yz}$ 1	$3d_{yz}$ 2	$3d_{x^2-y^2}$ 1	$3d_{x^2-y^2}$ 2	$3d_{xy}$ 1	$3d_{xy}$ 2
1	a_g	CC-$\sigma(s)$	−41.23	0.42	−0.42	−1.00	1.00	0.05	−0.05	−0.02	−0.02
2	b_u	CC-$\sigma(s)$	−39.80	0.00	0.00	−0.01	0.01	0.01	−0.01	0.06	−0.06
3	a_u	CC-$\sigma(s)$	−36.70	0.46	0.46	0.92	0.92	−0.12	−0.12	0.01	0.01
4	b_g	CC-$\sigma(s)$	−34.58	0.00	0.00	0.00	0.00	0.00	0.00	0.11	−0.11
5	a_g	CH-σ	−28.97	−0.07	0.07	0.08	−0.08	0.13	−0.13	−0.02	−0.02
6	b_u	CH-σ	−27.44	0.00	0.00	0.00	0.00	0.00	0.00	−0.21	−0.21
7	b_u	CH-σ	−24.50	0.00	0.00	0.00	0.00	0.00	0.00	−0.01	−0.01
8	a_g	CH-σ	−24.06	0.52	−0.52	−0.07	0.07	−0.37	0.37	−0.01	−0.01
9	a_u	CH-σ	−22.36	0.02	0.02	0.36	0.36	−0.45	−0.45	0.00	0.00
10	b_g	CH-σ	−21.72	0.00	0.00	0.00	0.00	0.00	0.00	0.11	0.11
11	a_u	CH-σ	−19.64	0.00	0.00	0.00	0.00	0.00	0.00	−0.20	−0.20
12	b_g	CH-σ	−19.53	−0.68	0.68	−0.48	−0.48	0.00	0.00	0.00	0.00
13	a_g	CC-$\sigma(p)$	−17.07	−0.15	0.15	0.22	−0.22	−0.25	0.25	0.00	0.00
14	b_u	CH-σ	−16.86	0.00	0.00	0.00	0.00	0.00	0.00	0.36	−0.36
15	a_g	CH-σ	−15.86	−0.32	0.32	0.72	−0.72	−0.11	0.11	0.02	0.02
16	b_u	CH-σ	−15.77	0.00	0.00	0.00	0.00	0.00	0.00	−0.16	0.16
17	a_g	CC-$\pi(\pi_1)$	−14.55	0.09	−0.09	0.66	−0.66	−0.02	0.02	0.03	0.03
18	a_u	CC-$\sigma(p)$	−14.27	−0.11	−0.11	−0.24	−0.24	0.16	0.16	0.00	0.00
19	b_g	CC-$\sigma(p)$	−14.18	0.00	0.00	−0.01	0.01	0.00	0.00	−0.20	−0.20

Table 5 (*cont.*)

MO	Γ_i	MO-Type	ε_i^{HT}	Coupling constants							
				$3d_{z^2}$ 1	$3d_{z^2}$ 2	$3d_{yz}$ 1	$3d_{yz}$ 2	$3d_{x^2-y^2}$ 1	$3d_{x^2-y^2}$ 2	$3d_{xy}$ 1	$3d_{xy}$ 2
20	a_u	CC-$\sigma(p)$	−13.59	0.00	0.00	0.00	0.00	0.00	0.00	0.14	−0.14
21	b_g	CH-σ	−13.40	0.03	0.03	0.21	0.21	−0.02	−0.02	0.00	0.00
22	a_g	CH-σ	−13.39	0.00	0.00	0.00	0.00	0.00	0.00	0.05	0.05
23	b_u	CH-σ	−13.26	0.01	−0.01	0.64	−0.64	−0.21	0.21	0.01	0.01
24	b_u	CC-$\pi(\pi_1)$	−12.73	0.00	0.00	0.01	−0.01	−0.01	0.01	−0.08	0.08
25	a_u	CC-$\pi(\pi_2)$	−12.22	0.08	0.08	0.97	0.97	−0.28	−0.28	0.00	0.00
26	*loc*	$3d_{z^2}(Ni_1)$	−11.51	—	[a]						
27	*loc*	$3d_{z^2}(Ni_2)$	−11.51	[a]	—						
28	*loc*	$3d_{yz}(Ni_1)$	−11.48			—	[a]				
29	*loc*	$3d_{yz}(Ni_2)$	−11.48			[a]	—				
30	b_g	CC-$\pi(\pi_2)$	−11.48	0.00	0.00	−0.01	−0.01	0.01	0.01	−0.07	−0.07
31	*loc*	$3d_{x^2-y^2}(Ni_1)$	−11.45					—	[a]		
32	*loc*	$3d_{x^2-y^2}(Ni_2)$	−11.45					[a]	—		
33	*loc*	$3d_{xy}(Ni_1)$	−11.44							—	[a]
34	*loc*	$3d_{xy}(Ni_2)$	−11.44							[a]	—
35	b_u	$3d_{xz}$, CC-$\pi(\pi_2)$	−11.20	0.00	0.00	0.00	0.00	0.00	0.00	0.03	0.03
36	b_g	$3d_{xz}$, CC-$\pi(\pi_2)$	−9.04	0.00	0.00	0.01	−0.01	0.01	−0.01	−0.38	−0.38
37	a_g	CC-$\pi(\pi_3)$	−8.75	−0.04	0.04	−0.12	0.12	0.01	0.01	−0.06	−0.06

[a] The Ni_1Ni_2 interaction constants are collected in a separate Table (Table 6).

Table 6. Coupling constants between the $3d$ AOs of the two Ni centers in bis(π-pentadienyl)dinickel according to an INDO calculation; all values in cm^{-1}

AO-Pair	Coupling constant
$3d_{z^2}$	89
$3d_{yz}$	90
$3d_{x^2-y^2}$	197
$3d_{xy}$	243

within the "through space" parameters is realized. The largest direct coupling elements are calculated for $3d_{x^2-y^2}$ and $3d_{xy}$ which have their maximum AO amplitudes in the region of the NiNi distance vector (σ and π interaction). A significant reduction is found for the δ pairs ($3d_{z^2}$ and $3d_{yz}$). The "through space" integrals for the coupling between Ni $3d$ functions of different angular quantum number are less than 10 cm^{-1}.

8. The Time Evolution of an Initially Prepared Ni $3d$ Hole-State

The matrix elements summarized in Tables 5 and 6 were used for the investigation of the time evolution of an initially prepared hole-state (Ni_1). The probability of hole propagation between the following instationary electron-hole pairs have been studied:

$(Hole\text{-}State)_1$	→	$(Electron\text{-}State)_2$	
$(3d_{z^2})_1$	→	$(3d_{z^2})_2$	(82)
$(3d_{x^2-y^2})_1$	→	$(3d_{x^2-y^2})_2$	(83)
$(3d_{xy})_1$	→	$(3d_{xy})_2$	(84)
$(3d_{yz})_1$	→	$(3d_{yz})_2$	(85)
$(3d_{z^2})_1$	→	$(3d_{x^2-y^2})_2$	(86)
$(3d_{z^2})_1$	→	$(3d_{yz})_2$	(87)
$(3d_{z^2})_1$	→	$(3d_{xy})_2$	(88)
$(3d_{yz})_1$	→	$(3d_{x^2-y^2})_2$	(89)
$(3d_{yz})_1$	→	$(3d_{xy})_2$	(90)
$(3d_{x^2-y^2})_1$	→	$(3d_{xy})_2$	(91)

Characteristic times of localization of the initially prepared hole-state are given in Table 7. An independent electron model has been assumed ($k = 1$ in Eq. (81)). This means that an unreorganized vacancy at Ni_1 has been prepared. In the fourth column of Table 7 $T_{c.50}$ for the processes (82)–(91) is given; this is the time necessary for the hole equibrilation between the time-dependent evoluting states localized at the Ni centers. With exception of the transfer process (88) $T_{c.50}$ spans a range between $3.56 \cdot 10^{-16}$ sec (85) to $1.41 \cdot 10^{-14}$ sec (86) and $1.45 \cdot 10^{-13}$ sec (91). Even in the independent electron model an interval for

Table 7. Times of hole propagation for Ni $3d$ hole-states; in the first column the transfer process for the hole migration is given. $T_{c.n}$ means that the localized hole-state at Ni_1 has been compensated by n% due to the electron-state of Ni_2 for a given electron-hole pair (e.g. $T_{c.10}$ = hole amplitude at Ni_1 is reduced by 10%). The times of hole propagation were observed in the framework of an independent electron model, the one-electron energies of the electron- and hole-state are the same. $T_{c.n}$ in sec

	$(AO)_1 \rightarrow (AO)_2$	$T_{c.10}$	$T_{c.30}$	$T_{c.50}$
1	$(3d_{z^2})_1 \rightarrow (3d_{z^2})_2$	$3.05 \cdot 10^{-15}$	$5.30 \cdot 10^{-15}$	$6.85 \cdot 10^{-15}$
2	$(3d_{x^2-y^2})_1 \rightarrow (3d_{x^2-y^2})_2$	$1.86 \cdot 10^{-15}$	$3.25 \cdot 10^{-15}$	$4.18 \cdot 10^{-15}$
3	$(3d_{xy})_1 \rightarrow (3d_{xy})_2$	$1.62 \cdot 10^{-15}$	$2.81 \cdot 10^{-15}$	$3.60 \cdot 10^{-15}$
4	$(3d_{yz})_1 \rightarrow (3d_{yz})_2$	$1.57 \cdot 10^{-16}$	$2.76 \cdot 10^{-16}$	$3.56 \cdot 10^{-16}$
5	$(3d_{z^2})_1 \rightarrow (3d_{x^2-y^2})_2$	$6.58 \cdot 10^{-15}$	$1.02 \cdot 10^{-14}$	$1.41 \cdot 10^{-14}$
6	$(3d_{z^2})_1 \rightarrow (3d_{yz})_2$	$1.76 \cdot 10^{-15}$	$2.59 \cdot 10^{-15}$	$3.22 \cdot 10^{-15}$
7	$(3d_{z^2})_1 \rightarrow (3d_{xy})_2$	[a]		
8	$(3d_{yz})_1 \rightarrow (3d_{x^2-y^2})_2$	$9.68 \cdot 10^{-16}$	$1.31 \cdot 10^{-15}$	$1.50 \cdot 10^{-15}$
9	$(3d_{yz})_1 \rightarrow (3d_{xy})_2$	$2.27 \cdot 10^{-14}$	$3.51 \cdot 10^{-14}$	$4.33 \cdot 10^{-14}$
10	$(3d_{x^2-y^2})_1 \rightarrow (3d_{xy})_2$	$4.93 \cdot 10^{-14}$	$8.39 \cdot 10^{-14}$	$1.45 \cdot 10^{-13}$

[a] Transfer probability too small that the hole migration takes place under adiabatical conditions.

the different equibrilation times of 10^3 is predicted. Within the selected model (unreorganized hole-domain) the fast transfer events do not couple with molecular phonons. In the limit of the slow hole migrations ($T_{c.50} > 10^{-14}$ sec) the Fröhlich interaction cannot be neglected. Here the possibility of nonadiabatical transfer events and a potential breakdown of the Born–Oppenheimer approximation must be taken into account.

The hole-propagation (88) is an exception in the studied series as the "tunnel integrals" are too small to allow hole tunneling on the adiabatical surface by purely electronic effects. In Fig. 4 the probability of hole propagation for this (88) electron-hole pair is displayed; $S_{ij}(t)$ is plotted for a time interval of 800 au (atomic units, 1 au = $1.94 \cdot 10^{-14}$ sec). $S_{ij}(t)$ does not exceed $6.0 \cdot 10^{-3}$. The coupling elements in Table 5 indicate that there is no ligand messenger state that interacts significantly both with the hole- and particle-component of the $\rho_i|\rho_j$ pair.

The calculated $T_{c.n}$ parameters of Table 7 should be compared with lifetimes of instationary localized states in other molecules (theoretical models based on an independent electron picture). In organic molecules lifetimes of π- and σ-vacancies of 10^{-16} sec have been calculated [52]. The core-hole exchange in acetylene requires $7 \cdot 10^{-15}$ sec [53], the lifetimes of K-states in Ar and C amount $1.3 \cdot 10^{-15}$ sec [54] and $1.3 \cdot 10^{-14}$ sec respectively [55].

In Tables 8–16 the contributions from the individual transfer channels for (82)–(91) are summarized.

The hole propagation in the case of the $(3d_{z^2})_1/(3d_{z^2})_2$ pair is predominantly submitted via CH-σ orbitals; 92.7% of the net probability of hole propagation

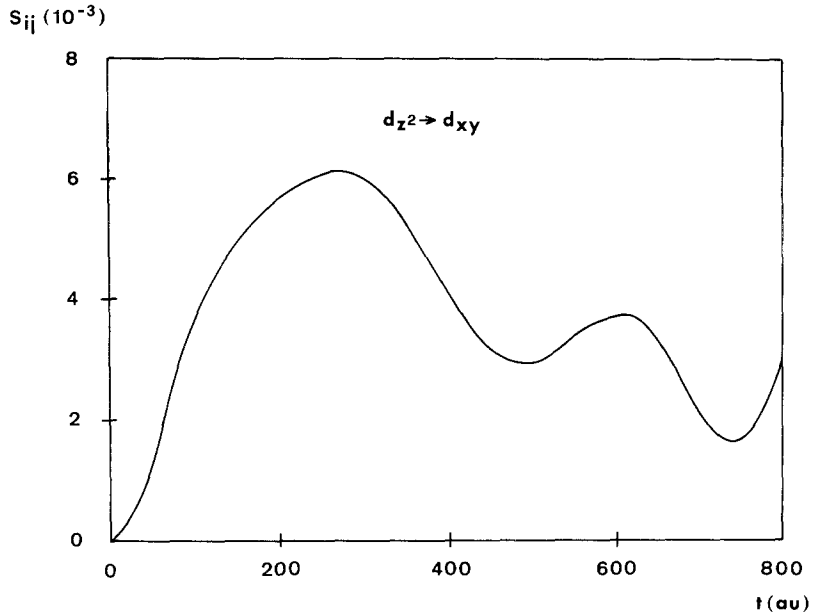

Fig. 4. Probability of hole propagation for the electron-hole pair $(3d_{z^2})_1$ (hole-state) → $(3d_{xz})_2$ (electron-state)

Table 8. Transfer channels for the $(3d_{z^2})_1/(3d_{z^2})_2$ electron-hole pair

Messenger MO	MO-Type	Contribution %
1	CC-σ	0.8
3	CC-σ	1.6
8	CH-σ	10.1
12	CH-σ	70.4
13	CC-σ	0.4
15	CH-σ	12.2
17	CC-π	0.1
18	CC-σ	0.4
25	CC-π	1.4
direct	$(3d_{z^2})_2$	2.6

Transfer channel	Contribution %
CC-σ	3.2
CH-σ	92.7
σ total	95.5
CC-π	1.5
ligand total	97.4
direct	2.6

Table 9. Transfer channels for the $(3d_{x^2-y^2})_1/(3d_{x^2-y^2})_2$ electron-hole pair

Messenger MO	MO-Type	Contribution %
8	CH-σ	1.0
9	CH-σ	2.7
13	CC-σ	1.0
15	CH-σ	0.1
18	CC-σ	0.7
23	CH-σ	5.2
25	CC-π	84.4
direct	$(3d_{x^2-y^2})_2$	4.9

Transfer channel	Contribution %
CC-σ	1.7
CH-σ	9.0
σ total	10.7
CC-π	84.4
ligand total	95.1
direct	4.9

Table 10. Transfer channels for the $(3d_{xy})_1/(3d_{xy})_2$ electron-hole pair

Messenger MO	MO-Type	Contribution %
11	CH-σ	0.2
14	CH-σ	3.5
16	CH-σ	0.2
19	CC-σ	1.4
20	CC-σ	0.4
24	CC-π	0.2
30	CC-π	65.8
35	$(3d_{xz}$, CC-$\pi)$	0.1
36	$(3d_{xz}$, CC-$\pi)$	22.8
direct	$(3d_{xy})_2$	5.5

Transfer channel	Contribution %
CC-σ	1.7
CH-σ	3.9
σ total	5.6
CC-π	66.0
CC-$\pi/3d_{xz}$	22.9
ligand total	94.5
direct	5.5

Table 11. Transfer channels for the $(3d_{yz})_1/(3d_{yz})_2$ electron-hole pair

Messenger MO	MO-Type	Contribution %
1	CC-σ	0.1
3	CC-σ	0.1
15	CH-σ	0.8
17	CC-π	1.2
23	CH-σ	3.2
25	CC-π	94.6
direct	$(3d_{yz})_2$	<0.1

Transfer channel	Contribution %
CC-σ	0.2
CH-σ	4.0
σ total	4.2
CC-π	95.8
ligand total	100.0
direct	<0.1

Table 12. Transfer channel for the $(3d_{z^2})_1/(3d_{x^2-y^2})_2$ electron-hole pair

Messenger MO	MO-Type	Contribution %
3	CC-σ	0.4
8	CH-σ	18.5
13	CC-σ	3.6
15	CH-σ	5.0
18	CC-σ	3.1
23	CH-σ	0.2
25	CC-π	69.2
direct	$(3d_{x^2-y^2})_2$	<0.1

Transfer channel	Contribution %
CC-σ	7.1
CH-σ	23.7
σ total	30.8
CC-π	69.2
ligand total	100.0
direct	<0.1

Table 13. Transfer channels for the $(3d_{z^2})_1/(3d_{yz})_2$ electron-hole pair

Messenger MO	MO-Type	Contribution %
1	CC-σ	1.0
3	CC-σ	1.4
12	CH-σ	7.7
13	CC-σ	0.2
15	CH-σ	14.0
17	CC-π	1.6
18	CC-σ	0.4
23	CH-σ	0.1
25	CC-π	73.6
direct	$(3d_{yz})_2$	<0.1

Transfer channel	Contribution %
CC-σ	3.0
CH-σ	21.8
σ total	24.8
CC-π	75.2
ligand total	100.0
direct	<0.1

Table 14. Transfer channels for the $(3d_{yz})_1/(3d_{x^2-y^2})_2$ electron-hole pair

Messenger MO	MO-Type	Contribution %
9	CH-σ	0.2
13	CC-σ	0.1
15	CH-σ	0.3
18	CC-σ	0.2
23	CH-σ	7.3
25	CC-π	91.9
direct	$(3d_{x^2-y^2})_2$	<0.01

Transfer channel	Contribution %
CC-σ	0.3
CH-σ	7.8
σ total	8.1
CC-π	91.9
ligand total	100.0
direct	<0.01

are due to these ligand MOs. CC-σ functions, π orbitals and the direct channel contribute with 3.2, 1, 5 and 2.6% to the transfer process.

The time evolution of the remaining electron-hole pairs profits in the first place from ligand π orbitals as messenger states. In the $(3d_{x^2-y^2})$ pair 84.4% of the net probability of hole propagation is due to pentadienyl π combinations. In any case small contributions from the direct interaction between the Ni centers, compared to the indirect coupling, are obtained.

A significant hole redistribution at the Ni centers is predicted for the evoluting pairs $(3d_{xy})_1/(3d_{xy})_2$ and $(3d_{x^2-y^2})_1/(3d_{xy})_2$. Here an important contribution to the net probability of hole propagation is due to the channel $(3d_{xz}, \text{CC-}\pi)$; the first step in the transfer therefore is an intraatomic redistribution of the hole-density [electron-density in (91)] from the $3d_{xy}$ AO into $3d_{xz}$ strongly coupled to the π system of the organic ligands.

The π contribution to the transfer process is largest for the $(3d_{yz})_1/(3d_{yz})_2$ electron-hole pair (95.8%). Significant ligand σ contributions (CH-σ) in addition to the $(3d_{z^2})$ pair are encountered in the two mixed transfer events (86) and (87) where the prepared hole-state corresponds to the $(3d_{z^2})_1$ AO.

Table 15. Transfer channels for the $(3d_{yz})_1/(3d_{xy})_2$ electron-hole pair

Messenger MO	MO-Type	Contribution %
1	CC-σ	0.1
15	CH-σ	1.2
17	CC-π	5.7
19	CC-σ	0.2
23	CH-σ	0.7
25	CC-π	1.8
30	CC-π	88.3
36	$(3d_{xz}, \text{CC-}\pi)$	0.5
37	CC-π	1.5
direct	$(3d_{xy})_2$	<0.1

Transfer channel	Contribution %
CC-σ	0.3
CH-σ	1.9
σ total	2.2
CC-π	97.3
CC-$\pi/3d_{xz}$	0.5
ligand total	100.0
direct	<0.1

Table 16. Transfer channels for the $(3d_{x^2-y^2})_1/(3d_{xy})_2$ electron hole pair

Messenger MO	MO-Type	Contribution %
5	CH-σ	0.2
8	CH-σ	1.0
9	CH-σ	0.2
13	CC-σ	0.1
15	CH-σ	0.8
17	CC-π	0.1
23	CH-σ	2.3
24	CC-π	1.1
25	CC-π	4.2
30	CC-π	69.6
35	($3d_{xz}$, CC-π)	0.1
36	($3d_{xz}$, CC-π)	19.9
37	CC-π	0.4
direct	$(3d_{xy})_2$	<0.1

Transfer channel	Contribution %
CC-σ	0.1
CH-σ	4.5
σ total	4.6
CC-π	75.4
CC-$\pi/3d_{xz}$	20.0
ligand total	100.0
direct	<0.1

Table 17. Times of hole propagation for the $(3d_{z^2})_1/(3d_{z^2})_2$ electron-hole pair as function of the reorganizational strength parameter $(1-k)$. See legend Table 7

$(1-k)$	$T_{c.10}$	$T_{c.30}$	$T_{c.50}$
0.000	$3.05 \cdot 10^{-15}$	$5.30 \cdot 10^{-15}$	$6.85 \cdot 10^{-15}$
0.010	$3.07 \cdot 10^{-15}$	$5.32 \cdot 10^{-15}$	$6.89 \cdot 10^{-15}$
0.025	$3.12 \cdot 10^{-15}$	$5.35 \cdot 10^{-15}$	$6.92 \cdot 10^{-15}$
0.050	$3.19 \cdot 10^{-15}$	$5.39 \cdot 10^{-15}$	$6.92 \cdot 10^{-15}$
0.075	$3.27 \cdot 10^{-15}$	$5.52 \cdot 10^{-15}$	$6.97 \cdot 10^{-15}$
0.100	$3.39 \cdot 10^{-15}$	$5.83 \cdot 10^{-15}$	$6.92 \cdot 10^{-15}$
0.125	$3.82 \cdot 10^{-15}$	$6.27 \cdot 10^{-15}$	$6.94 \cdot 10^{-15}$
0.150	[a]		

[a] The transfer probability is too small that the migration takes place under adiabatical conditions.

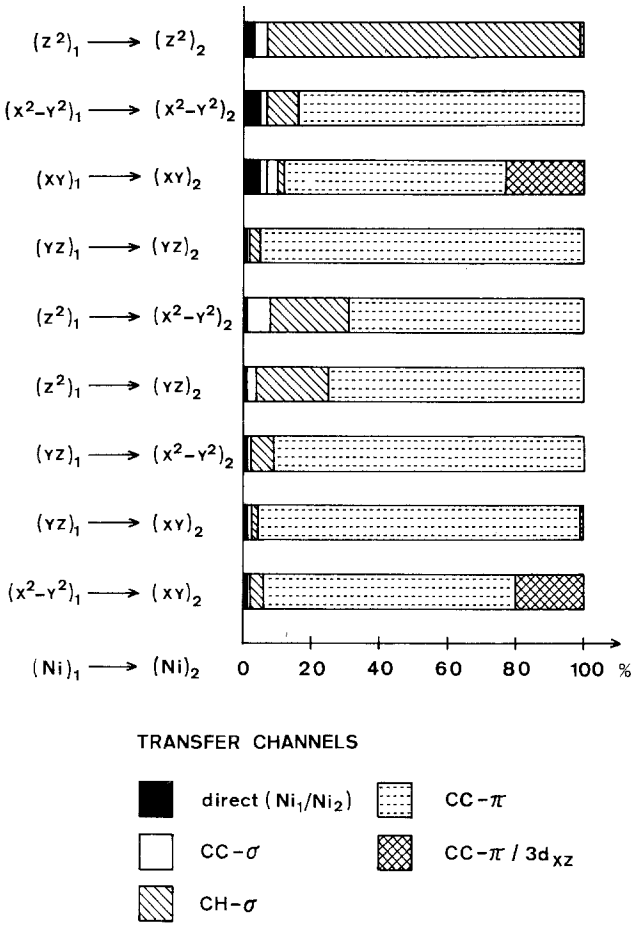

Fig. 5. Fragmentation into the individual transfer channels (direct, CC-σ, CH-σ, CC-π and CC-$\pi/3d_{xz}$) for the nine possible combinations of electron-hole pairs leading to a purely electronical transfer probability

In Fig. 5 the different transfer channels for the calculated electron-hole combinations are summarized schematically. The most important messenger states are displayed in Fig. 6. The MOs 8, 12 and 15 are CH-σ combinations, 25 and 26 ligand π functions and 36 the delocalized linear combination of the Ni $3d_{xz}$ carbon multicenter bonds; this messenger orbital requires the intraatomic hole-reorganization at the Ni sides.

In Table 17 the variation of the $T_{c.n}$ parameters of the $(3d_{z^2})_1/(3d_{z^2})_2$ electron-hole pair is shown if the ith hole-domain is modified due to reorganizational rearrangements. $(1-k)$ in Eq. (81) is a measure of the deviation from a Koopmans' analogue approximation. The $T_{c.n}$ parameters are enlarged with increasing $(1-k)$ values. Up to $(1-k)=0.125$ only small variations are predicted. If $(1-k)$ is enlarged furthermore, the probability of hole propagation is too small that a

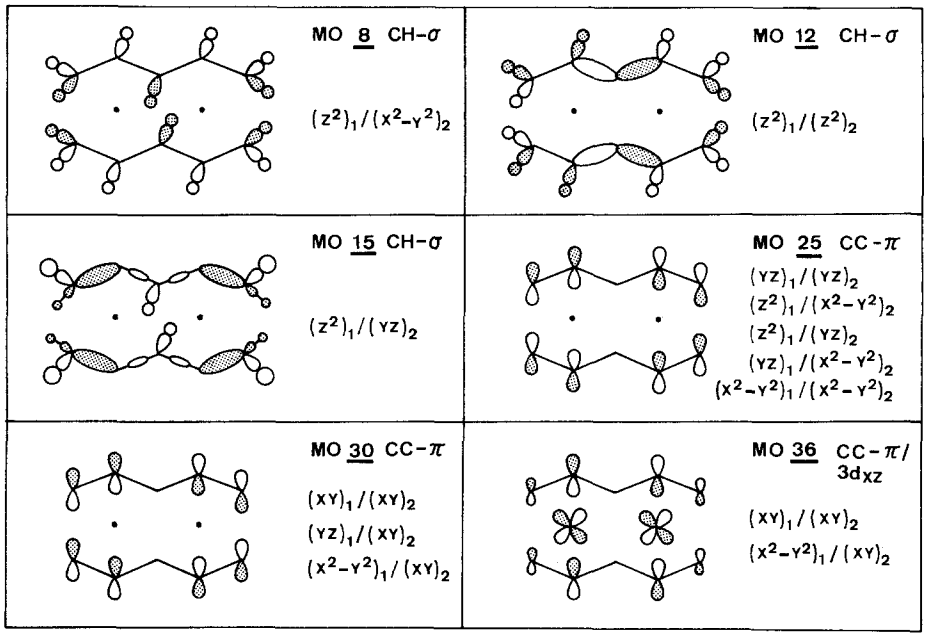

Fig. 6. Schematical representation of the most important messenger orbitals of the pentadienyl ligands

transfer event is possible on the adiabatic surface by purely electronical effects; the coupling to molecular vibrations is the necessary condition for the hopping event.

In Fig. 7 the probability of hole propagation for the $(3d_{z^2})$ pair is displayed for reorganizational strength parameters $(1-k)$ of 0.125 and 0.100. Both probability amplitudes are comparable up to a time interval to 10 au. For the amplitude with the 0.125 factor than an oscillatory behaviour is calculated (maximum of $S_{ij}(t) = 0.10$). On the other side the transfer event closer to the independent electron limit allows the hole-propagation by purely electronic effects. In Fig. 8 the oscillation of $S_{ij}(t)$ for a $(1-k)$ value of 0.5 is shown; the transfer probability is reduced furthermore.

With increasing reorganization in the ith hole-domain the probability of hole propagation is reduced, the transfer times are enlarged. At a critical value of the reorganization strength parameter the electron (hole) propagation becomes impossible by purely electronic effects. Here only the vibrational components of the Hamiltonian (H_v, $H_{el\text{-}v}$) allow the hopping event.

9. Conclusion

The purely electronical aspects of electron (hole) propagation in the binuclear Ni complex **1** have been investigated. A Fock operator of the Hubbard-type is constructed from first principles starting from the canonical molecular orbitals

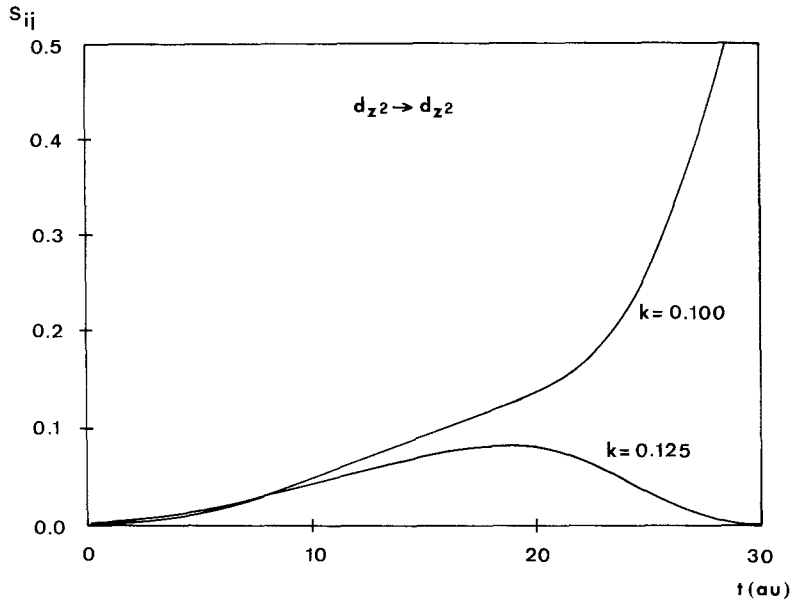

Fig. 7. Probability of hole propagation for the electron-hole pair $(3d_{z^2})_1 \rightarrow (3d_{z^2})_2$ as function of the reorganization strength $(1-k)$

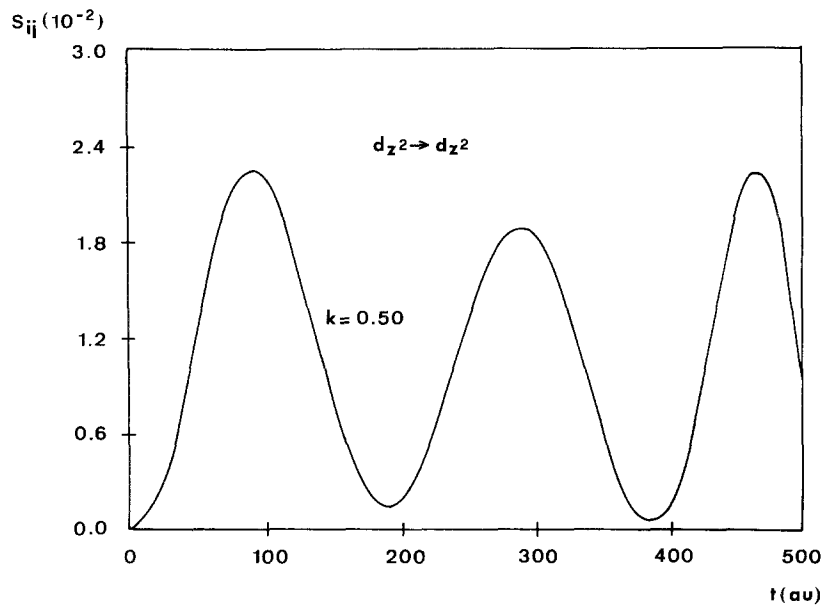

Fig. 8. Probability of hole propagation for the electron-hole pair $(3d_{z^2})_1 \rightarrow (3d_{z^2})_2$ with a strength parameter 0.50 for hole-reorganizations

of an ordinary HF calculation; the CMO's are transformed into a one-electron basis suitable for the study of time-dependent phenomena. The transfer Fockian allows the study of electron (hole) propagation of the HF SCF level.

By means of the Δ_i potential it is possible to mimic reorganizational rearrangements in the ith hole-domain and thus to modify the initial conditions for the transfer process. In the present model the time-evoluting electron-hole pair is dynamically coupled by means of the Δ_i potential. The computational results obtained for **1** have shown that the probability of electron (hole) migration depends critically on the initially prepared conditions in the instationary hole-domain. The predicted transfer times span a wide range from fast processes that are not coupled to molecular phonons to the limit where the electronic tunnel probability is too small to allow a transfer event. In these cases an extended theoretical treatment under the inclusion of the vibrational motions is necessary that conserves the methodical careness of the electronic aspects discussed in the present work.

Appendix A

In this appendix two important choices for suitable one-electron bases, Hilpert spaces mounted to these bases as well as the associated transfer-type Fock operators are presented. Additionally the probability amplitudes and the probabilities of hole propagation are given. The necessary Fock matrices are displayed schematically, their formulation exactly parallels the steps discussed in Sects. 2 and 4.

(a) Initial condition: hole-state localized at ρ_i, hole propagation into the instationary donor states ρ_j and ρ_k (irreversible ansatz).

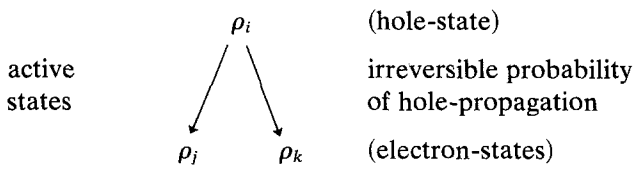

messenger states $(N-3)$: γ_l $\quad (l \neq i, j, k)$

Time-dependent one-electron basis:

$$|\phi_0(t)\rangle = A\{\rho_i(1, t)\rho_j(2, t)\rho_k(3, t)\gamma_1(4) \cdots \gamma_{(N-3)}(N)\}. \tag{A1}$$

Hilbert space: $L_1^N(t) = L_i(t) + L_j(t) + L_k(t) + L_1^{(N-3)}$. (A2)

Decoupled localized Fockian $F^{\mathrm{LMO}}_{(i,j,k)\mathrm{dec}}$: Transfer Fockian of the Hubbard-type:

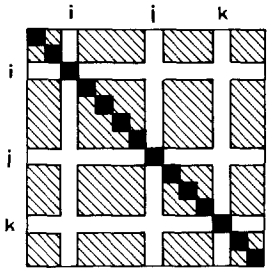

Scheme 3

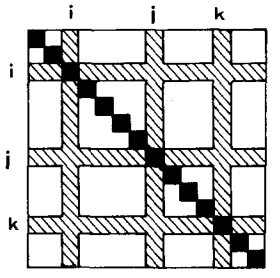

Scheme 4

Probability of hole propagation:

$$S_{ij}(t) = |U_{ij}|^2 \tag{A3}$$

$$S_{ik}(t) = |U_{ik}|^2. \tag{A4}$$

Probability amplitude $P_i(t)$:

$$\begin{aligned} P_i(t) &= |U_{ij}|^2 P_j(0) + |U_{ik}|^2 P_k(0) \\ &= S_{ij}(t) P_j(0) + S_{ik}(t) P_k(0). \end{aligned} \tag{A5}$$

In (A5) the RPA has been used.

(b) Initial condition: hole-state localized at ρ_i, transfer (direct) to ρ_j and to ρ_k, secondary hole propagation from ρ_j to ρ_k; all steps are irreversible.

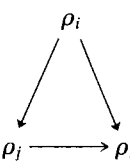

active states

ρ_i (hole-state)

irreversible probability of hole-propagation

$\rho_j \longrightarrow \rho_k$ (electron-states)

messenger states $(N-3)$: $\gamma_l \qquad (l \neq i, j, k)$.

The time-dependent one-electron basis, the mounted Hilbert space as well as $F^{\mathrm{LMO}}_{(i,j,k)dec}$ and F^{HT} correspond to (a).

Probability of hole propagation:

$$S_{ij}(t) = |U_{ij}|^2 \tag{A6}$$

$$S_{ik}(t) = |U_{ik}|^2 \tag{A7}$$

$$S_{jk}(t) = |U_{jk}|^2. \tag{A8}$$

Probability amplitudes $P_i(t)$ and $P_j(t)$:

$$P_i(t) = S_{ij}(t) P_j(0) + S_{ik}(t) P_k(0) \tag{A9}$$

$$P_j(t) = P_j(0) + S_{jk}(t) P_k(0) - S_{ij}(t) P_j(0). \tag{A10}$$

Appendix B

For the determination of c_i in Eq. (79) we performed a series of perturbational calculations according to Eq. (80) to determine reorganizational increments Δ_i for electron removal. In the case of strongly localized MOs Δ_i is proportional to the fourth power of the LCAO coefficient of the AOs forming the localized domain in the ith one-electron state. Extrapolation to the full localized limit allows the calculation of c_i in (79).

The one-center self-energy terms must be determined in a way that the design of the molecular Hamiltonian is properly taken into account (*ab initio* vs. semiempirical procedure). In the case of the used INDO approximation [16] experimental one-center integrals of Sichel and Whitehead [56] and DiSipio and

coworkers [57] ($3d$ centers) represent this suitable choice. In the present work $c_i = 0.22$ has been determined.

Eq. (79) only holds if a single atomic orbital ρ_i is forming the ith localized domain ($3d$ AO, lone-pair). In the case of decoupled bonds or even more delocalized fragments (79) must be substituted by Eqs. (B1) or (B2).

Decoupled bond with the AOs φ_ν and φ_μ in ρ_i

$$\Delta_i = c_i(c^4_{\mu i} j_{\mu\mu} + c^4_{\nu i} j_{\nu\nu}). \tag{B1}$$

Molecular fragment with n decoupled AOs φ_n in ρ_i

$$\Delta_i = c_i(c^4_{\mu i} j_{\mu\mu} + c^4_{\mu i} j + \cdots c^4_{ni} j) \tag{B2}$$

$$j_{\mu\mu} = \left\langle \varphi_\mu(1)\varphi_\mu(2) \left| \frac{1}{r_{12}} \right| \varphi_\mu(1)\varphi_\mu(2) \right\rangle. \tag{B3}$$

In the case of (79) obviously the identity (B4) is true

$$\rho_i(1) = \varphi_i(1). \tag{B4}$$

$c_{\mu i}$ is the μth AO coefficient in the ith decoupled localized domain. It is clearly seen that the calculated Δ_i potentials are reduced with increasing delocalization of ρ_i.

Acknowledgment. The work has been supported by the Stiftung Volkswagenwerk. The assistance of Mrs. H. Wellnitz and Mrs. I. Grimmer in the preparation of the manuscript is gratefully acknowledged.

References

1. Harriman, J. E., Maki, A. H.: J. Chem. Phys. **39**, 778 (1963)
2. Taylor, H. V., Allred, A. L., Hoffman, B. M.: J. Am. Chem. Soc. **95**, 3215 (1973)
3. Goodings, E. P.: Chem. Soc. Rev. **5**, 95 (1976)
4. Robin, M., Day, P.: Adv. Inorg. Radiochem. **10**, 248 (1967)
5. Cowan, D. O., LeVanda, C., Park, J., Kaufman, F.: Acc. Chem. Res. **6**, 1 (1973); Taube, H.: Pure Appl. Chem. **44**, 25 (1976); Goldanskii, V. I.: Acc. Chem. Res. **10**, 153 (1977)
6. Haim, A.: Acc. Chem. Res. **8**, 264 (1975)
7. Taube, H.: Electron transfer reactions of complex ions in solution. New York: Academic Press 1970
8. Wang, J. H.: Acc. Chem. Res. **3**, 90 (1970)
9. Hopfield, J. J.: Proc. Natl. Acad. Sci. USA **71**, 3640 (1974)
10. Grimes, C. J., Piszkiewicz, D., Fleischer, E. B.: Proc. Natl. Acad. Sci. USA **71**, 1408 (1974)
11. Creutz, C., Sutin, N.: Proc. Natl. Acad. Sci. USA **72**, 2858 (1975)
12. Schumacher, E.: Chimia **32**, 193 (1978); Calzaferri, G.: Chimia **32**, 241 (1978)
13. Rienäcker, R., Yoshida, H.: Angew. Chem. **81**, 708 (1969)
14. Krüger, C.: Angew. Chem. **81**, 708 (1969)
15. Bogdanović, B., Yus, M.: Angew. Chem. **91**, 742 (1979); Bogdanović, B., Krüger, C., Kuzmin, O.: Angew. Chem. **91**, 744 (1979)
16. Böhm, M. C., Gleiter, R.: Theoret. Chim. Acta (Berl.) **59**, 127 (1981)

17. Hoffmann, R., Imamura, A., Hehre, W. J.: J. Am. Chem. Soc. **90**, 1499 (1968); Hoffmann, R.: Acc. Chem. Res. **4**, 1 (1971); Gleiter, R.: Angew. Chem. **86**, 770 (1974)
18. Fröhlich, H., Pelzer, H., Zienau, S.: Phil. Mag. **41**, 221 (1950)
19. Møller, C., Plesset, M. S., Phys. Rev. **46**, 618 (1934)
20. Anachenkov, V. I., Leontyev, V. B.: Int. J. Quantum. Chem. **17**, 265 (1980)
21. De Vault, D., Chance, B.: Biophys. J. **6**, 825 (1966); De Vault, D., Parks, J. H., Chance, B.: Nature **215**, 642 (1967); Hales, B. J.: Biophys. J. **16**, 471 (1976); v. Heuvelen, A.: Biophys. J. **16**, 939 (1976); Petrov, E. G.: Int. J. Quantum. Chem. **16**, 133 (1979); Chance, B., Markus, R. A., De Vault, D. C., Schriffer, J. R., Frauenfelder, H., Sutin, N., eds.: Tunneling in biological systems. New York: Academic Press 1979
22. Förster, T.: Naturwissenschaften **33**, 166 (1946); Dexter, D. L.: J. Chem. Phys. **21**, 836 (1953)
23. Jortner, J.: J. Chem. Phys. **64**, 4860 (1976); Ulstrup, J., Jortner, J.: J. Chem. Phys. **63**, 4358 (1975); Jortner, J., Ulstrup, J.: J. Am. Chem. Soc. **101**, 3744 (1979)
24. Levich, V. G., Dogonadze, R. R.: Collect. Czech. Chem. Commun. **26**, 193 (1961)
25. Van Duyne, R. P., Fischer, S. F.: Chem. Phys. **5**, 183 (1974)
26. Ulstrup, J.: Charge transfer processes in condensed media, Lecture notes in chemistry, Vol. **10**, and references cited therein. Berlin: Springer Verlag 1979
27. Piepho, S. B., Krausz, E. R., Schatz, P. N.: J. Am. Chem. Soc. **100**, 2996 (1978); Wong, K. Y., Schatz, P. N., Piepho, S. B.: J. Am. Chem. Soc. **101**, 2793 (1979); Schatz, P. N., Piepho, S. B., Krausz, E. R.: Chem. Phys. Letters **55**, 539 (1978); Wong, K. Y., Schatz, P. N.: Chem. Phys. Letters **71**, 152 (1980)
28. Christov, S. G.: Ber. Bunsenges. Phys. Chem. **79**, 357 (1975)
29. Hubbard, J.: Proc. Roy. Soc. A **238**, 4 (1963); Proc. Roy. Soc. A **277**, 237 (1964); Proc. Roy. Soc. A **281**, 401 (1964)
30. Ondrechen, M. J., Ratner, M. A.: J. Chem. Phys. **66**, 938 (1977); Ondrechen, M. J., Ratner, M. A.: Chem. Phys. Letters **51**, 573 (1977); Ondrechen, M. J., Ratner, M. A., Sabin, J. R.: J. Chem. Phys. **71**, 2244 (1979)
31. Halpern, J., Orgel, L. E.: Dis. Faraday Soc. **29**, 32 (1960)
32. Kanamori, J.: Prog. Theor. Phys. **30**, 275 (1963); Goodenough, J. B.: J. Appl. Phys. **37**, 1415 (1966)
33. Ratner, M. A., Ondrechen, M. J.: Mol. Phys. **32**, 1233 (1976); Ratner, M. A.: Int. J. Quantum Chem. **14**, 675 (1978)
34. Dirac, P. A. M.: Proc. Roy. Soc. A **114**, 243 (1927); Dirac, P. A. M.: Principles of quantum mechanics. Oxford: Oxford University Press 1958
35. Löwdin, P.-O.: Adv. Quantum Chem. **3**, 323 (1967)
36. Messiah, A.: Quantum mechanics. Amsterdam: North Holland 1962; Zülicke, L.: Quantenchemie, Vol. **1**, Grundlagen und allgemeine Methoden. Berlin: VEB Deutscher Verlag der Wissenschaften 1973
37. Kauzmann, W.: Quantum chemistry. New York: Academic Press 1957
38. Koopmans, T.: Physica **1**, 104 (1933)
39. Heilbronner, E., Schmelzer, A.: Helv. Chim. Acta **58**, 936 (1975)
40. Peeters, D., Leroy, G., Rosoux-Clarisse, F. in: Recent advances in the quantum theory of polymers, Lecture Notes in Physics, Vol. **113**, Berlin: Springer Verlag 1980
41. Edmiston, C., Ruedenberg, K.: Rev. Mod. Phys. **35**, 457 (1963); Edmiston, C., Ruedenberg, K.: J. Chem. Phys. **43**, 597 (1965); Ruedenberg, K. in: Modern quantum chemistry, Vol. **1**. New York: Academic Press 1965
42. Foster, J. M., Boys, S. F.: Rev. Mod. Phys. **32**, 300 (1960); Boys, S. F.: Rev. Mod. Phys. **32**, 296 (1960)
43. v. Niessen, W.: J. Chem. Phys. **56**, 4249 (1972); v. Niessen, W.: Theoret. Chim. Acta (Berl.) **27**, 9 (1972)
44. Magnasco, V., Perico, A.: J. Chem. Phys. **47**, 971 (1967); J. Chem. Phys. **48**, 800 (1968)
45. Slater, J. C., Mann, J. B., Wilson, T. M., Wood, J. H.: Phys. Rev. **184**, 672 (1969); Slater, J. C.: Adv. Quantum. Chem. **6**, 1 (1972)
46. Goscinski, O., Pickup, B. T., Purvis, G.: Chem. Phys. Letters **22**, 167 (1973)
47. Gopinathan, M. S.: J. Phys. B **12**, 521 (1979)

48. Böhm, M. C.: Thesis, TH Darmstadt, Federal Republic of Germany 1980
49. Cederbaum, L. S.: Theoret. Chim. Acta (Berl.) **31**, 239 (1973)
50. Mulliken, R. S.: J. Chem. Phys. **23**, 1833, 2343 (1955)
51. Wiberg, K. B.: Tetrahedron **24**, 1083 (1968)
52. Spehr, R., Schnabl, H.: Z. Naturforsch. **28a**, 1729 (1973); Spehr, R.: Z. Naturforsch. **35a**, 876 (1980)
53. Snyder, L. C.: J. Chem. Phys. **55**, 95 (1971)
54. Paratt, L. C.: Rev. Mod. Phys. **31**, 616 (1959)
55. McGuire, E. J.: Phys. Rev. **185**, 1 (1969)
56. Sichel, J. M., Whitehead, A.: Theoret. Chim. Acta (Berl.) **7**, 32 (1967)
57. Di Sipio, L., Tondello, E., De Michelis, G., Oleari, L.: Chem. Phys. Letters **11**, 287 (1971)

Received July 20, 1981